

AEDC-TR-73-36

cy3

MAR 2 1973  
APR 2 1973  
SEP 12 1975  
MAR 15 1982  
SEP 14 1989

**INVESTIGATION OF THE EFFECTS OF  
NOSE BLUNTNES ON NATURAL AND INDUCED  
BOUNDARY-LAYER TRANSITION ON  
AXISYMMETRIC BODIES IN SUPERSONIC FLOW**



**Jack D. Coats**

**ARO, Inc.**

**February 1973**

Approved for public release; distribution unlimited.

**VON KÁRMÁN GAS DYNAMICS FACILITY  
ARNOLD ENGINEERING DEVELOPMENT CENTER  
AIR FORCE SYSTEMS COMMAND  
ARNOLD AIR FORCE STATION, TENNESSEE**

Property of U. S. Air Force  
AEDC LIBRARY  
F40600-73-C-0004

# ***NOTICES***

When U. S. Government drawings specifications, or other data are used for any purpose other than a definitely related Government procurement operation, the Government thereby incurs no responsibility nor any obligation whatsoever, and the fact that the Government may have formulated, furnished, or in any way supplied the said drawings, specifications, or other data, is not to be regarded by implication or otherwise, or in any manner licensing the holder or any other person or corporation, or conveying any rights or permission to manufacture, use, or sell any patented invention that may in any way be related thereto.

Qualified users may obtain copies of this report from the Defense Documentation Center.

References to named commercial products in this report are not to be considered in any sense as an endorsement of the product by the United States Air Force or the Government.

INVESTIGATION OF THE EFFECTS OF  
NOSE BLUNTNES ON NATURAL AND INDUCED  
BOUNDARY-LAYER TRANSITION ON  
AXISYMMETRIC BODIES IN SUPERSONIC FLOW

Jack D. Coats  
ARO, Inc.

Approved for public release; distribution unlimited.

## FOREWORD

The research presented herein was done by the Arnold Engineering Development Center (AEDC), Air Force Systems Command (AFSC), Arnold Air Force Station, Tennessee, under Program Element 65402234.

The data were obtained by ARO, Inc. (a subsidiary of Sverdrup & Parcel and Associates, Inc.), contract operator of AEDC, AFSC. The work was conducted under ARO Project No. VT0747, and the manuscript was submitted for publication on July 21, 1970.

This report also was submitted to the University of Tennessee Space Institute in partial fulfillment of the requirements for a Master of Science Degree.

The author would like to express his appreciation to Mr. L. Pfaff who was instrumental in accomplishing all phases of the experimental program and to Mr. J. D. Whitfield, Mr. C. J. Schueler, and Mr. H. W. Ball of ARO, Inc., and the AEDC, United States Air Force for their permission to use the experimental data. Dr. J. C. Adams and Mr. E. O. Marchand were most helpful in providing computer programs for obtaining theoretical predictions of the boundary-layer and the surrounding inviscid flow-field characteristics. The advice of Mr. J. L. Potter throughout the analysis of the test results and the preparation of the report has been a major contribution and is greatly appreciated.

This technical report has been reviewed and is approved.

A. L. COAPMAN  
Colonel, USAF  
Director of Test

**ABSTRACT**

A series of tests has been conducted at free-stream Mach numbers four and eight to determine the effectiveness of three-dimensional boundary-layer trips in promoting transition on very blunt axisymmetric bodies with near equilibrium wall temperatures. Temperature distributions obtained with temperature sensing gages inserted in the model surface were used to locate boundary-layer transition at Mach number four, and qualitative results, based on pitot pressure measurements, were obtained at Mach number eight. A simple modification of a technique proposed by van Driest and Blummer for determining an effective trip size for blunt bodies is shown to yield a correlation applicable to their data on a sphere at Mach number two and the present configurations at Mach number four. The present data are also shown to be in agreement with the two-dimensional zero pressure gradient trip sizing correlation developed by Potter and Whitfield which has the distinct advantage of providing not only the necessary trip size but also the resulting location of boundary-layer transition.

## CONTENTS

	<u>Page</u>
ABSTRACT . . . . .	iii
NOMENCLATURE . . . . .	vi
I. INTRODUCTION . . . . .	1
II. APPARATUS	
2.1 Wind Tunnels . . . . .	6
2.2 Models . . . . .	7
2.3 Instrumentation . . . . .	10
III. EXPERIMENTAL TECHNIQUE	
3.1 Test Procedure . . . . .	10
3.2 Data Uncertainty . . . . .	11
IV. RESULTS . . . . .	11
V. CONCLUDING REMARKS . . . . .	44
REFERENCES . . . . .	49

## ILLUSTRATIONS

Figure

1. Model Details . . . . .	8
2. Temperature Sensing Gage . . . . .	9
3. Surface Temperature Distributions with Natural Transition at $M_\infty = 4$ . . . . .	12
4. Comparison of Experimental and Theoretical Pitot Pressure Profiles at $M_\infty = 4$ . . . . .	14
5. Entropy Variation Normal to Model Surface at $M_\infty = 4$ . . . . .	17
6. Natural Transition Reynolds Number at $M_\infty = 4$ . . . . .	19
7. Surface Temperature Distributions with Induced Transition at $M_\infty = 4$ . . . . .	20
8. Variation of Boundary-Layer Transition with Free-Stream Unit Reynolds Number, $M_\infty = 4$ . . . . .	23
9. Variation of Boundary-Layer Transition with Local Unit Reynolds Number, $M_\infty = 4$ . . . . .	26
10. Comparison of the Present Blunt Body Results at $M_\infty = 4$ with the Potter and Whitfield Zero Pressure Gradient Correlation . . . . .	29

<u>Figure</u>	<u>Page</u>
11. Variation of the Transition Reynolds Number with Trip Diameter Reynolds Number . . . . .	31
12. Comparison of the Present Data with the Results and Correlation of van Driest and Blummer. . . . .	34
13. Comparison of the Present Data and the Results of van Driest and Blummer with the Modified Correlation . . . . .	35
14. Comparison of Laminar Boundary-Layer Pitot Pressure Profiles with Theoretical Estimates at $M_\infty = 8$ , $Re_\infty/in. = 0.19 \times 10^6$ . . . . .	37
15. Effect of Boundary-Layer Trips ( $k = 0.125$ in., $x_k = 4.73$ in. on the Development of Pitot Pressure Profiles for the Hemisphere-Cylinder at $M_\infty = 8$ , $Re_\infty/in. = 0.19 \times 10^6$ . . . . .	40
16. Pitot Pressure Profiles on the Sphere-Cone-Cylinder at Station $x_p = 31.80$ , $M_\infty = 8$ , $Re_\infty/in. = 0.19 \times 10^6$ . . . . .	45
17. Pitot Pressure Profiles on the Hemisphere-Cylinder at $x_p = 25.79$ , $M_\infty = 8$ , $Re_\infty/in. = 0.19 \times 10^6$ . . . . .	47
18. Pitot Pressure Profiles for the Compound Sphere-Cylinder at $x_p = 25.15$ in., $M_\infty = 8$ , $Re_\infty/in. = 0.19 \times 10^6$ . . . . .	48

### NOMENCLATURE

b	Leading-edge diameter of hollow cylinder model (Fig. 6), in.
D	Model diameter, in.
K	Total trip height above model surface, ( $k + t$ ), in.
k	Spherical trip diameter, in.
$k_{eff}$	Spherical trip diameter that produces the minimum transition Reynolds number, in.
M	Mach number
$M_{ch}$	Characteristic model surface Mach number
p	Pressure, psia

$p'_0$	Stagnation pressure behind a normal shock wave in the free stream, psia
$p_p$	Pitot pressure, psia
Re/in.	Unit Reynolds number per inch, $(\rho u/\mu)/12$
Re <sub>KK</sub>	Roughness height Reynolds number, $(Re_K/in.)K$
Re' <sub>K</sub>	$(Re_{KK})(T_K/T_w)^{0.5+\omega}$
Re <sub><math>\delta</math>x<sub>t</sub></sub>	Transition Reynolds number, $(Re_\delta/in.)x_t$
Re' <sub><math>\delta</math>k</sub>	Trip diameter Reynolds number, $(Re'_\delta/in.)k$
Re' <sub><math>\delta</math>x<sub>k</sub></sub>	Roughness position Reynolds number $(Re'_\delta/in.)x_k$
Re' <sub><math>\delta</math><math>\delta^*</math><sub>k</sub></sub>	Displacement thickness Reynolds number, $(Re'_\delta/in.)\delta^*_k$
S	Entropy, Btu/°R
T	Temperature, °R
t	Trip ring thickness, in.
u	Velocity, fps
x	Wetted distance along model surface measured from stagnation point, in.
x <sub>p</sub>	x at location of pitot pressure profile measurement, in.
y	Vertical distance above surface measured from surface, in.
$\gamma$	Ratio of specific heats of air
$\delta$	Total boundary-layer thickness, in.
$\delta^*$	Boundary-layer displacement thickness, in.
$\epsilon$	Value of Re' <sub>K</sub> where $x_t = x_k$
$\theta$	Bevel angle of hollow cylinder leading edge (Fig. 6), deg
$\mu$	Dynamic viscosity, $(lb)(sec)/(ft)^2$
$\rho$	Density, $(lb)(sec)^2/(ft)^4$
$\omega$	Exponent in viscosity - temperature relation

## SUBSCRIPTS

K	At height K in undisturbed laminar boundary layer at the boundary-layer trip
k	At axial station of the boundary-layer trip

o	Stagnation conditions
t	At boundary-layer transition
to	At transition on smooth model ( $K = 0$ )
w	Model surface conditions
$\delta$	At edge of the undisturbed laminar boundary layer
$\delta'$	$\delta$ at the boundary-layer trip
$\infty$	Free stream

### CONFIGURATION NOMENCLATURE

CS-C	Compound Sphere-Cylinder
H-C	Hemisphere-Cylinder
S-C-C	Sphere-Cone-Cylinder

## SECTION I INTRODUCTION

The reliability of wind tunnel data for predicting certain characteristics of full-scale flight vehicles, such as dynamic stability, drag, and heat transfer, often depends upon matching the location of boundary-layer transition on the model to that on the full-scale vehicle. The boundary layer on the flight vehicle is in many cases predominantly turbulent; however, at the comparatively low Reynolds numbers available in most wind tunnels, the boundary layer on the model may be primarily, if not entirely, laminar. To overcome this deficiency in wind tunnel data, it is frequently necessary to induce boundary-layer transition on the model through the use of boundary-layer trips.

Establishing criteria for selecting the best type of boundary-layer trip and the optimum size and location have been the objectives of many experimental investigations. Probably the most difficult and as yet generally unsolved phase of the problem has been to select a trip that would move transition to the desired location on the model surface but not disturb the surrounding flow to the extent that unwanted secondary effects arise. As in most studies to date, this phase of the problem was not considered in the present investigation. It must be noted, however, that any decision to use boundary-layer trips should be based on a careful evaluation of the test objectives to insure that the benefits of duplicating the turbulent boundary layer are not outweighed by the adverse effects of the trips.

In contrast to the extensive data available regarding boundary-layer trips for the zero pressure gradient case of flow over flat plates and cones, the problem of inducing transition on blunt bodies has received comparatively little systematic investigation. The preferred practice has been to conduct a trip study at the beginning of each wind tunnel test involving a blunt body when turbulent boundary layers were required. This is a good procedure and, whenever possible, it should be followed to insure a turbulent boundary layer even if an applicable trip sizing technique is used. For the reasons discussed below it is in many cases, however, an extreme complication to incorporate a blunt body trip study in the test plan.

On models with a sharp leading edge, confirmation of a turbulent boundary layer is a relatively simple matter, usually accomplished through flow visualization techniques such as schlieren or shadowgraph photographs. On blunt bodies, the boundary layer generally cannot be photographed satisfactorily with standard techniques, and one must

frequently revert to measurement of surface temperatures or heat transfer or other specialized methods for determining the nature of the boundary layer. Pitot pressure profiles are useful in detecting the onset of transition but are of limited value in transition studies since it is very difficult to differentiate between the profiles of transitional and fully developed turbulent boundary layers. Sublimation techniques, oil flow, temperature sensitive paints, and the recently proposed liquid crystals (Ref. 1) are satisfactory for transition detection in special cases; however, there are limitations with regard to model fabrication techniques, thermal conductivity, operating temperatures, etc.

A trip sizing study for a force or pressure test on a blunt body may therefore require special transition detection instrumentation, such as surface temperature or heat-transfer gages, hot wire probes, or hot film gages, and in some cases even a special model. The benefits of developing a reliable trip sizing technique for blunt bodies are thus obvious. The objective of this investigation was to provide some information applicable to very blunt bodies and by comparison with zero pressure gradient results and the limited data available from other blunt body trip studies, to evaluate the possibility of developing an appropriate trip sizing technique.

Until more blunt body data become available, the induced transition studies for the zero pressure gradient case must be relied upon to define the significant parameters. A review of the parameters advanced by various authors as being important in trip sizing indicates that the following list, compiled by Sterrett, Morrisette, Whitehead, and Hicks (Ref. 2) includes most of the significant factors affecting roughness induced boundary-layer transition:

1. Type of roughness.
2. Spacing of three-dimensional roughness.
3. Roughness position Reynolds number,  $Re_{\delta'x_k}$ .
4. Roughness height Reynolds number,  $Re_{\zeta k}$ .
5. Wall temperature.
6. Local Mach number.
7. Unit Reynolds number,  $Re/in$ .
8. Model configuration.
9. Pressure gradient.

Another factor noted by Holloway and Morrisette (Ref. 3) that should be added to this list is the wind tunnel because of its inherent free-stream turbulence level. It was shown by Pate and Schueler (Ref. 4) that radiated aerodynamic noise from the turbulent boundary layer on the tunnel wall was a primary factor affecting the natural transition Reynolds number on

a hollow cylinder test model. Since the radiated noise level is a function of tunnel size, the stability of the model boundary layer must change with tunnel size, and this would in turn be expected to alter at least the onset of induced boundary-layer transition. This factor was not individually examined in these tests. However, tunnel effects in general are accounted for in the Potter and Whitfield trip sizing correlation used in analysis of the test results (Section IV).

Van Driest and McCauley (Ref. 5) and Jackson and Czarnecki (Ref. 6) found that three-dimensional roughness elements were considerably more effective than two-dimensional trip wires of corresponding height. It was also noted by Potter and Whitfield (Ref. 7) that on the basis of their correlation parameters, three-dimensional roughness elements were more effective in supersonic flow than were corresponding two-dimensional trips, but they point out, as have other authors, that this is not the case in subsonic flow. Sterrett, Morrisette, Whitehead, and Hicks (Ref. 2) tested "pyramidal", "spherical", and "pinhead" roughness elements and noted an apparent increase in effectiveness with outward (away from the body) movement of the centroid of the three-dimensional trip frontal area. This suggests that spheres may not be the most effective type of three-dimensional trip; however, their availability in various sizes and the simplicity of spherical trip ring construction justifies their use until a clearly superior trip is found.

Klebanoff, Schubauer, and Tidstrom (Ref. 8) and van Driest and McCauley (Ref. 9) have investigated the radial spacing between three-dimensional roughness elements in subsonic and supersonic flow, respectively, and noted no change in effectiveness. McCauley, Saydah, and Bueche (Ref. 10) note an apparent decrease in trip effectiveness for a model on which they later found the trips had been erroneously spaced somewhat less than two diameters from center to center. They attributed the decreased effectiveness to inadequate trip spacing which resulted in the spheres acting as a two-dimensional trip. Van Driest and Blummer (Ref. 11) suggest that a center-to-center spacing of four diameters is adequate to eliminate trip interaction, and this seems to be a satisfactory and generally accepted "rule of thumb."

The significance of the roughness position Reynolds number ( $Re_{\delta^*x_k}$ ) in trip sizing studies is perhaps more obvious when it is recalled that this quantity is intimately related to the boundary-layer displacement thickness ( $\delta^*$ ). Dryden (Ref. 12) found that for two-dimensional roughness in low speed flows, the ratio of the trip height to the displacement thickness was a very satisfactory correlating parameter for the ratio of the natural to the induced transition Reynolds numbers. Klebanoff, Schubauer, and Tidstrom (Ref. 8), however, found the Dryden correlation

to be unsatisfactory for three-dimensional roughness elements in low speed flow. The roughness position Reynolds number corresponding to the minimum value of the transition Reynolds number was selected by van Driest and Blummer (Ref. 13) as a prime variable and appears in their two-dimensional roughness correlation curve, although in its final form the correlation is presented in terms of the displacement thickness Reynolds number and a temperature corrected  $k/\delta^*$  term. Sterrett, Morrisette, Whitehead, and Hicks (Ref. 2) support the conclusion of Braslow, Hicks, and Harris (Ref. 14) regarding the existence of a minimum roughness position Reynolds number and point out that it may be very hard to promote boundary-layer transition at the roughness elements, even with a large trip, if the roughness is located too close to the leading edge.

First recognition of the roughness height Reynolds number as a significant factor in trip effectiveness has been attributed to Schiller (Ref. 15). This parameter in the form proposed by Schiller, based on the local flow properties at the top of the trip in the undisturbed boundary layer or in slightly modified form based on the properties at the edge of the boundary layer, is probably the parameter most frequently found in trip sizing correlations. The early concept of a critical roughness height Reynolds number at which boundary-layer transition moved in one abrupt step from its natural transition location to the trip was proven to be in error by Fage (Ref. 16); however, somewhat modified definitions of a critical Reynolds number are still in use. For example, Braslow, Knox, and Horton (Refs. 17, 18, and 19) use "the value at which turbulent spots are initiated behind the roughness and at which only a small increase in roughness Reynolds number is required to move the fully developed turbulent boundary layer substantially up to the roughness elements" to define a critical roughness height Reynolds number.

The reduction in trip effectiveness with increasing wall temperature is very obvious in the sharp cone data of van Driest and Blummer (Ref. 13). McCauley, Saydah, and Bueche (Ref. 10) noted a significant decrease in trip effectiveness with increasing wall temperature and an apparent relationship between the growth in boundary-layer displacement thickness with increasing temperature and the decrease in trip effectiveness. Potter and Whitfield (Ref. 7) also account for wall temperature in their correlation; thus the significance of the model wall temperature as a parameter in trip sizing seems clearly established. The present tests were conducted entirely at near equilibrium wall temperatures; however, and temperature effects were not considered in the investigation.

The adverse effect of increasing Mach number on successfully tripping a laminar boundary layer has been clearly established in references previously noted (Refs. 2, 5, and 7), by Potter and Whitfield (Ref. 20) and by Whitfield and Iannuzzi (Ref. 21). It has been concluded by most authors that bringing boundary-layer transition to the trip is generally impractical at high Mach numbers. Sterrett, et al. (Ref. 2) proposed that the forward movement of transition to a position from 25 to 50 percent of its natural location was a realistic limit. McCauley, Saydah, and Bueche (Ref. 10) were unable to obtain natural transition locations in their experiments on sphere cones at Mach number 10 but noted that with boundary-layer trips the transition region, the end of which corresponded to the transition location, extended over the entire model length, a distance of approximately three feet.

It is well known that the natural transition Reynolds number, which is intimately related to the stability of the boundary layer, varies with the unit Reynolds number (Refs. 4, 7, and 20). Assuming, as in the discussion of aerodynamic noise, that the onset of induced transition is also dependent to some extent on the stability of the boundary layer, the unit Reynolds number would be expected to appear in analyses of induced transition data. The absence of this parameter may be the reason for the limited applicability of some trip sizing techniques. Potter and Whitfield (Ref. 7) account for unit Reynolds number effects by including the natural transition location ( $x_{t_0}$ ) in their correlation parameter. This seems to have particular merit since it not only accounts for unit Reynolds number effects within a single wind tunnel, it also adjusts the predicted induced transition location to account for the differences in transition locations of various wind tunnels.

The direct relationship between the model configuration and surface pressure gradients leads to simultaneous consideration of these parameters. A favorable pressure gradient is generally believed to delay transition while an adverse gradient tends to promote early boundary-layer transition. Since both favorable and adverse pressure gradients exist on a blunt body, the overall effect on natural transition is dependent on the body location at which transition occurs. The same can probably be said of induced transition since the effectiveness of a trip is dependent, at least to some extent, on conditions upstream and even downstream, as well as at the trip.

The strong bow shock wave produced by a blunt nose is a significant factor affecting both natural and induced transition. The shock wave reduces the local surface Mach number which tends to promote natural transition and make the boundary layer easier to trip; however, the adverse effect of the accompanying reduction in the local unit Reynolds

number far outweighs the Mach number influence, thereby delaying both natural and induced boundary-layer transition on slightly blunted bodies, i. e., up to a point where the effect of bluntness reverses.

The effect of the parameters discussed above on induced transition on blunt bodies is somewhat speculative since there has been comparatively little experimental investigation on bodies other than flat plates and cones. Holloway and Morrisette (Ref. 3) investigated blunt flat plates at Mach number 6; van Driest and Blummer (Ref. 13) conducted a brief study on spheres at Mach number 2; and McCauley, Saydah, and Bueche (Ref. 10) investigated sphere cones at Mach number 10. It is obvious that considerably more experimental investigation will be required before a trip sizing technique, generally applicable to all blunt bodies, can be considered completely reliable. The present work is an investigation of the trip sizing problem at near equilibrium temperatures on a series of very blunt bodies. It is hoped that, in addition to providing information within this very limited scope, the results will be useful in the eventual general solution of the problem of induced transition on blunt bodies.

## SECTION II APPARATUS

### 2.1 WIND TUNNELS

Supersonic Wind Tunnel (A) and Hypersonic Wind Tunnel (B) are continuous, closed-circuit, variable density wind tunnels. Tunnel A has an automatically driven flexible-plate-type nozzle with a 40- by 40-in. test section. The tunnel can be operated at Mach numbers from 1.5 to 6 at maximum stagnation pressures from 29 to 200 psia, respectively, and stagnation temperatures up to 750°R (Mach number 6). Minimum operating pressures range from about one-tenth to one-twentieth of the maximum at each Mach number.

The Tunnel A pitot pressure probe is supported from the tunnel sidewall. Using a remotely operated drive mechanism, the probe can be moved horizontally, normal to the model centerline, from its fully retracted position against the sidewall to any location up to the model surface. The system is equipped with a grounding light which indicates when the probe comes in contact with the model surface. The position recording equipment uses this contact point as a reference, thereby minimizing errors in the model-to-probe distance. The probe used for these tests was formed from 0.0275-in. -OD tubing with a 0.004-in. wall,

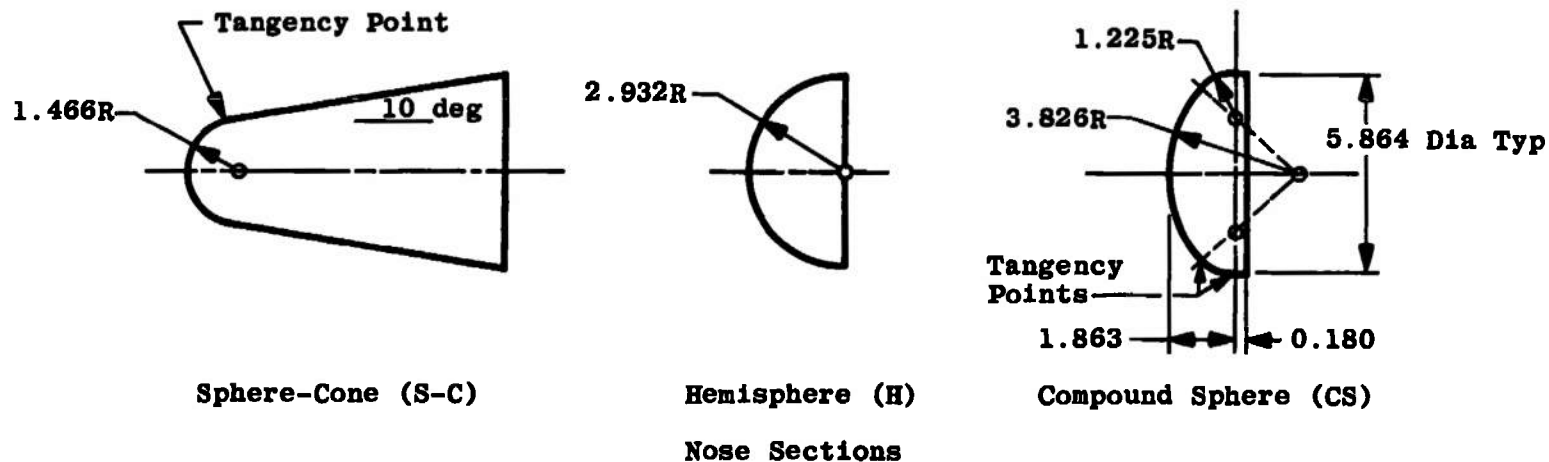
flattened to a total height of 0.017 in. The measured pressure was assumed to be that at the midpoint of the probe. There are no provisions for axial movement; thus all Tunnel A pitot pressure profiles were obtained at an axial station 14 in. forward of the model base.

Tunnel B has an axisymmetric contoured nozzle and a 50-in. -diam test section. The tunnel can be operated at nominal Mach number 8, at stagnation pressures from 50 to 900 psia, and stagnation temperatures up to 1350°R. The model may be injected into the tunnel for a test run and then retracted for model cooling or model changes without interrupting the tunnel flow. The Tunnel B pitot pressure probe system is mounted from the top of the tunnel and can be moved both vertically and horizontally by a remotely operated drive mechanism. This system is also equipped with a grounding light to indicate contact with model surface, and the probe used was similar to that described above for the Tunnel A tests.

## 2.2 MODELS

Details of the three interchangeable nose sections and the cylindrical body are given in Fig. 1. The model components were stainless steel with a wall thickness of approximately 0.25 in. The boundary-layer trips were stainless steel spheres spot welded at four diameter intervals to 0.25-in.-wide by 0.005-in.-thick steel bands contoured to fit the model surface. Most testing was done with the trip bands on the body at the nose-body junction; thus, the spheres, located at the center of the bands, were 0.125 in. downstream of the nose-body junction. Limited testing of the Sphere-Cone-Cylinder at Mach number 8 was done with the trip bands located on the cone at the sphere-cone junction.

The sensing element of the temperature gages (Fig. 2) consisted of a Chromel<sup>®</sup>-Alumel<sup>®</sup> thermocouple embedded in a cylindrical nylon insulator with the junction at the upper surface. The sensing element was pressed and cemented in a 0.250-in. -diam steel shell, which was in turn seated in a hole in the model such that the thermocouple junction was flush with the model surface. These gages provided reliable temperature distributions at Mach number 4; however, similar gages, modified slightly for high temperature operation, were found to be unsatisfactory for use in these models at Mach number 8. Their failure to provide reliable results at this higher Mach number was attributed to insufficient insulation of the thermocouple junction from the model in conjunction with the large heat capacity of the model, the low rate of heat input from the stream, and axial conduction along the model surface to the water-cooled sting.



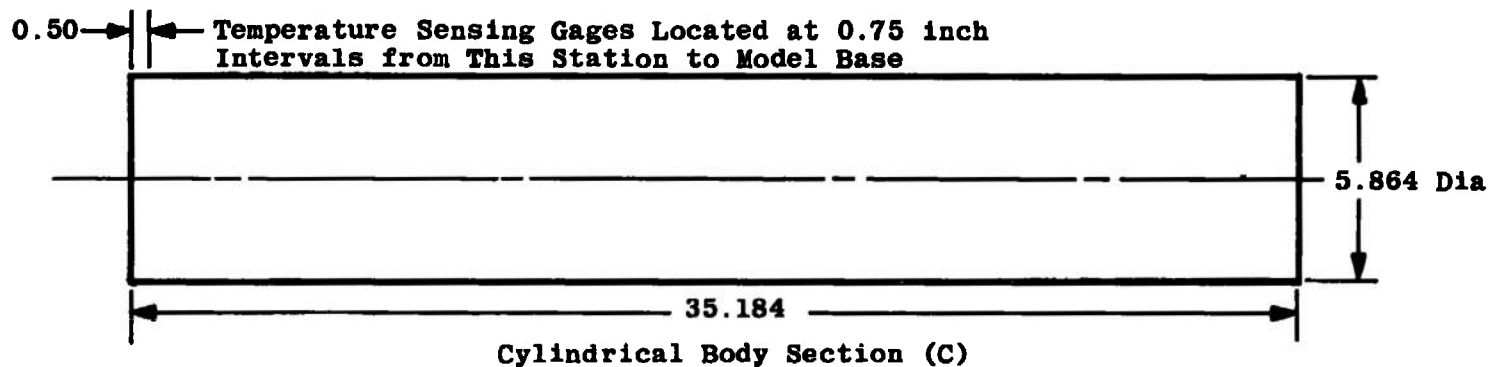
Sphere-Cone (S-C)

Hemisphere (H)

Compound Sphere (CS)

Nose Sections

8



Cylindrical Body Section (C)

All dimensions are in inches.

Fig. 1 Model Details

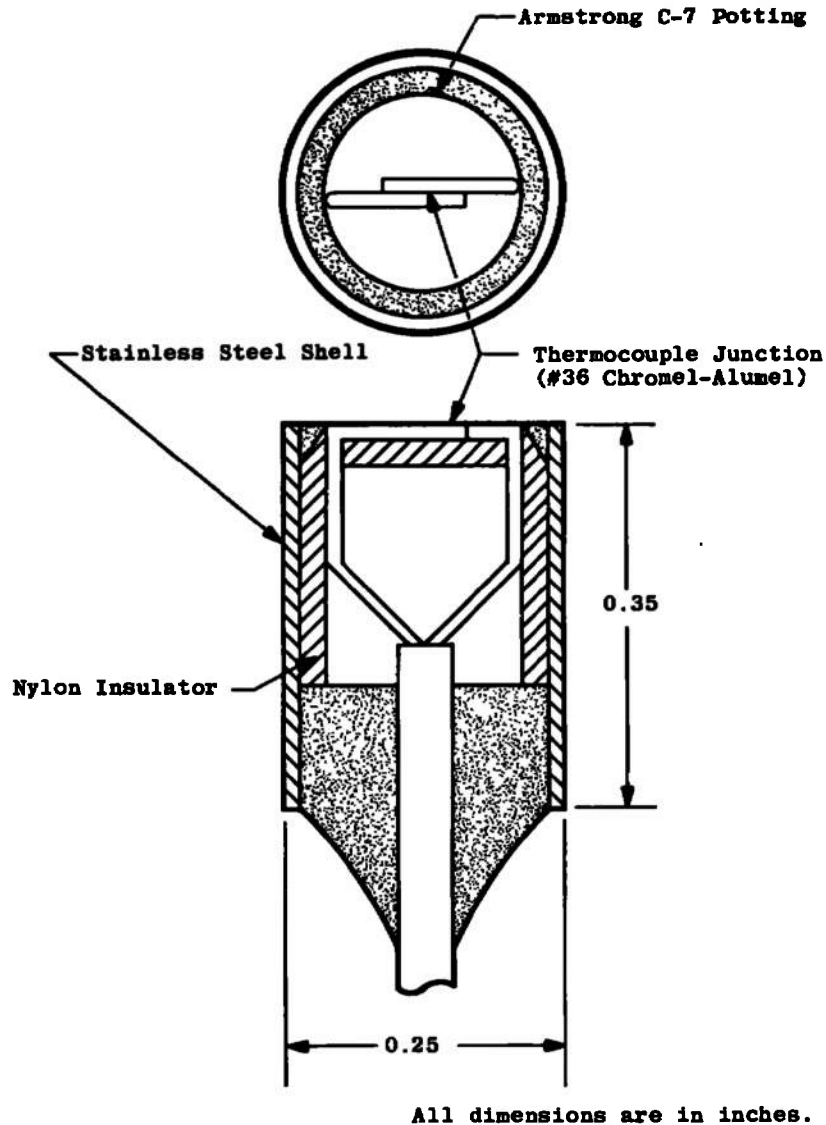


Fig. 2 Temperature Sensing Gage

Although considerable care was taken in fabrication of the temperature gages and in drilling the mounting holes in the model, some difficulty was encountered in maintaining a smooth surface along the ray of gages. After installation was complete, each gage was carefully stoned to insure that no edges extended above the model surface. Upon completion of this final contouring, measurements along the ray of gages showed that local irregularities generally did not exceed 0.002 in. The surface finish of the model, measured with a stylus having a radius of 0.005 in., ranged from 20 to 80  $\mu$ in. As others have pointed out, surface roughness measurements under such conditions obviously are of

limited value. The areas of the nose surrounding the stagnation point were roughened from erosion by small particles in the flow during extended periods of wind tunnel testing. No attempt was made to smooth these surfaces since it was the intent of the investigation to duplicate, as nearly as possible, conditions representative of those encountered in routine testing. Also, these effects are believed to be negligible in comparison to the influence of the much larger boundary-layer trips.

## 2.3 INSTRUMENTATION

The pitot pressures were measured with differential transducers referenced to a near vacuum which was monitored and included in the pressure calculations. These transducers and also those used to measure the stilling chamber pressure were calibrated before each operating shift to full-scale ranges compatible with the pressures to be measured. The reference junctions of the thermocouples in the temperature gages were maintained at 132°F. The millivolt outputs of the thermocouples were monitored and processed with a Beckman 210 multichannel analog-to-digital converter and recorder. The digitized temperature outputs and those of the pressure transducers and other tunnel information were recorded on paper tapes. All data reduction was accomplished on a Control Data Corporation 1604-B digital computer.

# SECTION III EXPERIMENTAL TECHNIQUE

## 3.1 TEST PROCEDURE

In Tunnel A, the normal procedure during the trip effectiveness studies was to increase the stagnation pressure until a visual display, proportional to the surface temperature distribution, indicated that the upstream movement of boundary-layer transition had ceased at a station very near the boundary-layer trips. Data were recorded at this condition and at a series of lower stagnation pressures, thereby defining the movement of boundary-layer transition with Reynolds number until transition moved off the model base. The natural transition data were obtained in the same manner except that the initial testing was done at the maximum Reynolds number available. Since the surface temperatures were providing reliable data, pitot pressure profiles were obtained at only a few representative test conditions. These were generally obtained prior to the temperature distributions in order to utilize the time required for stabilization of the surface temperatures.

After elimination of the temperature gages as a means of detecting boundary-layer transition at Mach number 8 in Tunnel B, a number of pitot pressure profiles were obtained in an attempt to gain some information regarding the effectiveness of the boundary-layer trips. Profiles were obtained at several axial stations primarily at Reynolds numbers of  $Re_{\infty}/in. = 0.19 \times 10^6$  and  $0.29 \times 10^6$ . The data were of rather limited value in this study because of the difficulty in interpreting the results. This will be discussed in more detail in Section IV.

### 3.2 DATA UNCERTAINTY

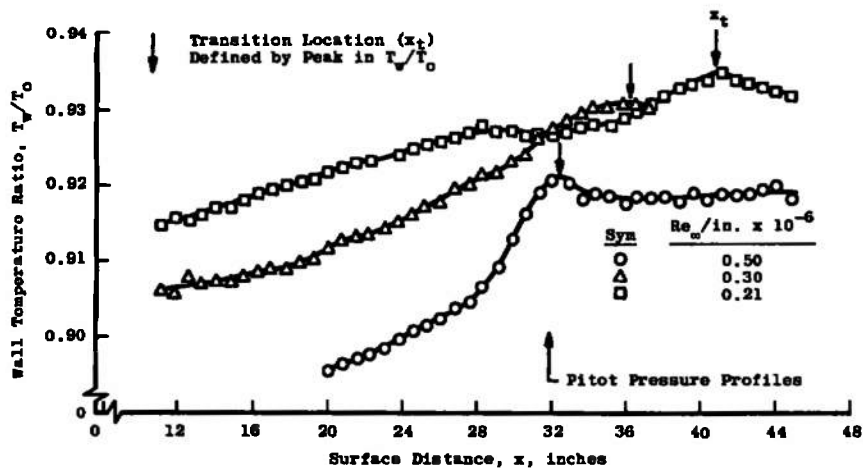
After completion of all assembly work, the thermocouples were connected to the recording equipment and the entire model was wrapped in asbestos. The model was allowed to soak to an equilibrium temperature which was assumed to be constant over the entire model after a period of twenty-four hours. The temperatures were recorded and the difference between each temperature and the overall mean was calculated and entered as a correction in the data reduction program. Since only the temperature distributions were important, this reduced the relevant error in the temperature data to that of the correction and the recording equipment, which is estimated to be approximately 1.5 deg overall and 0.3 deg between adjacent thermocouples.

The pitot pressures were measured with the standard tunnel pressure systems that can be calibrated to 1-, 5-, and 15-psid ranges. These systems are estimated to be accurate to within 0.3 percent of the range in use. The stagnation pressure and temperature are estimated to be accurate to 0.5 percent and 3 deg, respectively.

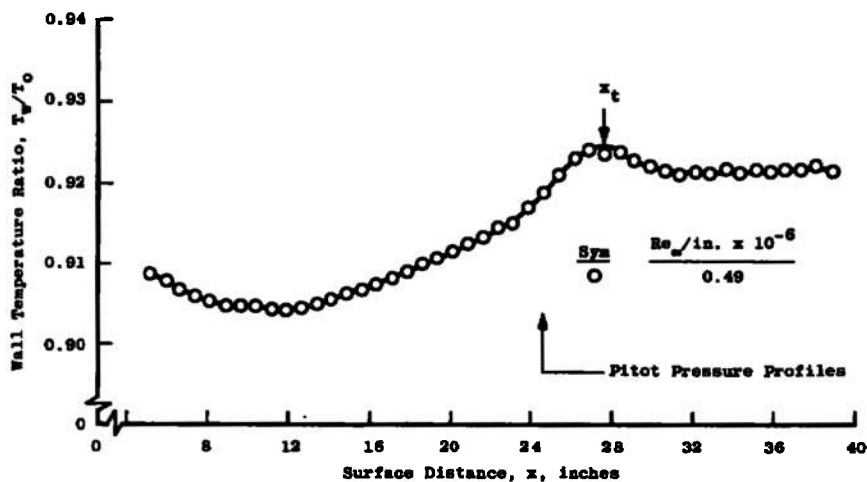
## SECTION IV RESULTS

Because reliable temperature data were obtained only at Mach number 4 and the temperatures provided the only available means of fixing the position of boundary-layer transition, emphasis must be placed on the test results at this lower Mach number. Some pitot pressure profiles obtained at Mach number 8 will be examined later in the discussion.

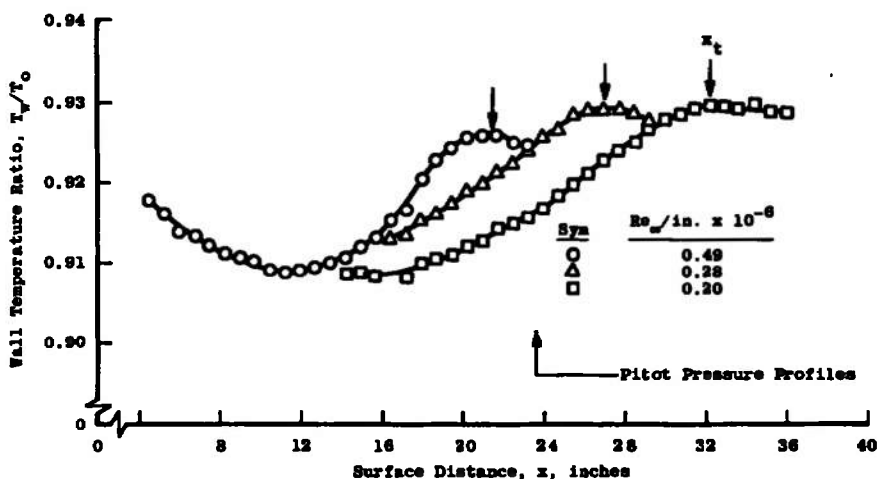
Surface temperature distributions illustrating natural transition on the three configurations without boundary-layer trips at Mach number 4 are presented in Fig. 3. The levels of the temperature in some cases appear to be inconsistent for different values of the free-stream Reynolds number.



a. Sphere-Cone-Cylinder



b. Hemisphere-Cylinder



c. Compound Sphere-Cylinder

Fig. 3 Surface Temperature Distributions with Natural Transition at  $M_\infty = 4$

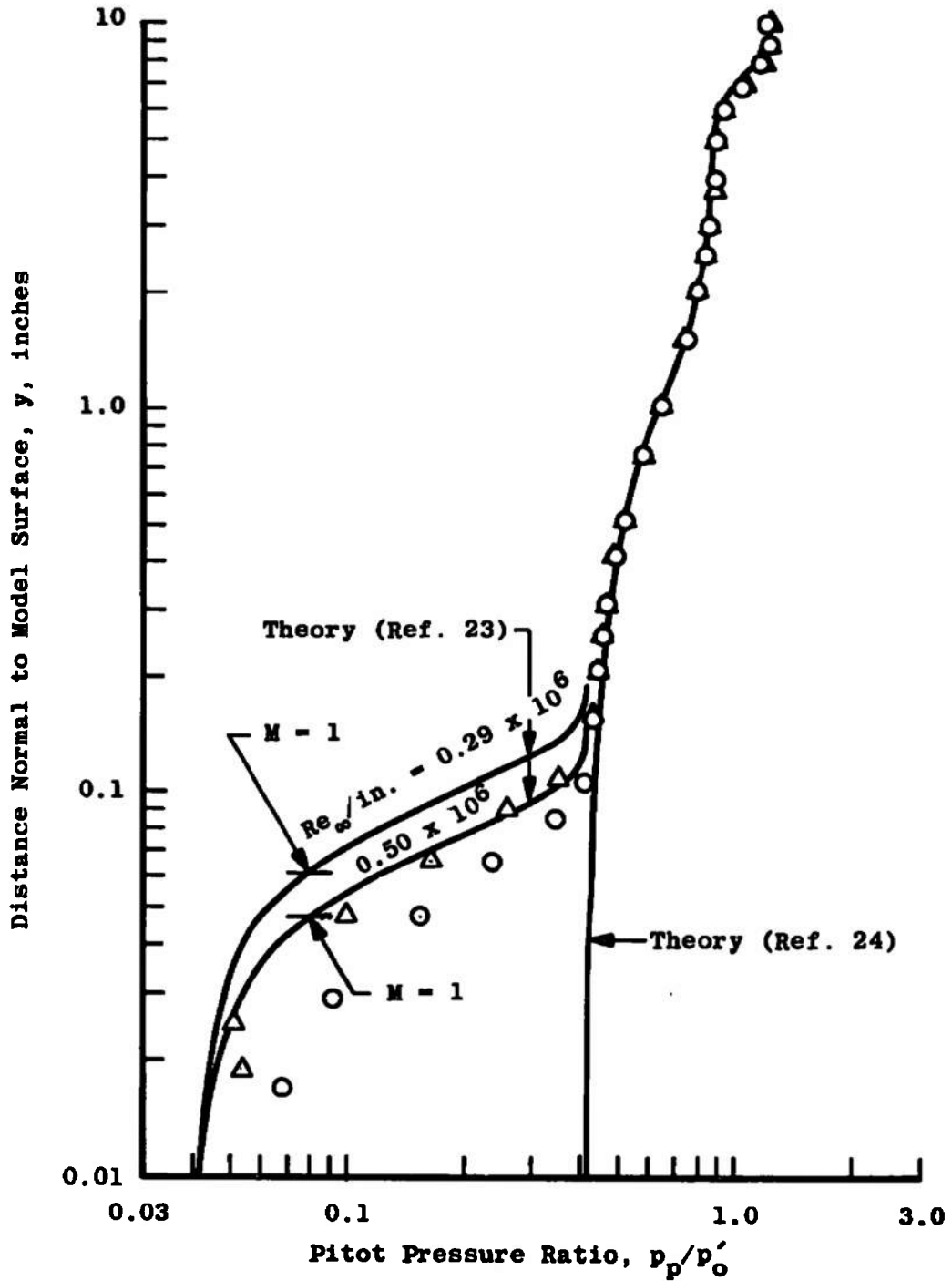
This is probably caused by the test technique since the data were recorded when a visual display of the temperatures showed a well-defined distribution with no evidence of local changes. In some cases this probably resulted in recording the data slightly before the equilibrium temperature was reached; however, the absence of local variations insured a fixed location of boundary-layer transition and no observable error in the test results.

Each distribution in Fig. 3 illustrates a peak model surface temperature, the center of which has been defined as the location of boundary-layer transition. The relationship between this temperature peak and the region over which transition takes place has been examined by Whitfield and Potter (Refs. 7 and 22) who concluded that the peak corresponded to the approximate center of a transition region defined by boundary-layer growth rates conforming to those of laminar  $[(\delta/x)^{0.5} = \text{const.}]$  and turbulent  $[(\delta/x)^{0.8} = \text{const.}]$  boundary layers. Although systematic data were not available on a single configuration, comparison of the limited pitot pressure profile data in Fig. 4 with the temperature distributions in Fig. 3 also indicates a gradual change from the laminar profile beginning upstream of the peak temperature and continuing to approach the characteristic near linear profile of a turbulent boundary layer for some distance downstream of the peak.

Comparison of the apparently laminar profile of the Sphere-Cone-Cylinder configuration at  $Re_{\infty}/\text{in.} = 0.29 \times 10^6$  (Fig. 4a) with the theoretical prediction of Adams (Ref. 23) suggests that the theory somewhat overestimates the actual boundary-layer thickness. This same tendency is evident, although to a lesser degree, in the Mach number 8 profiles to be discussed later. The general form of the pitot pressure profiles, on the other hand, appears to be well predicted by the theoretical estimates.

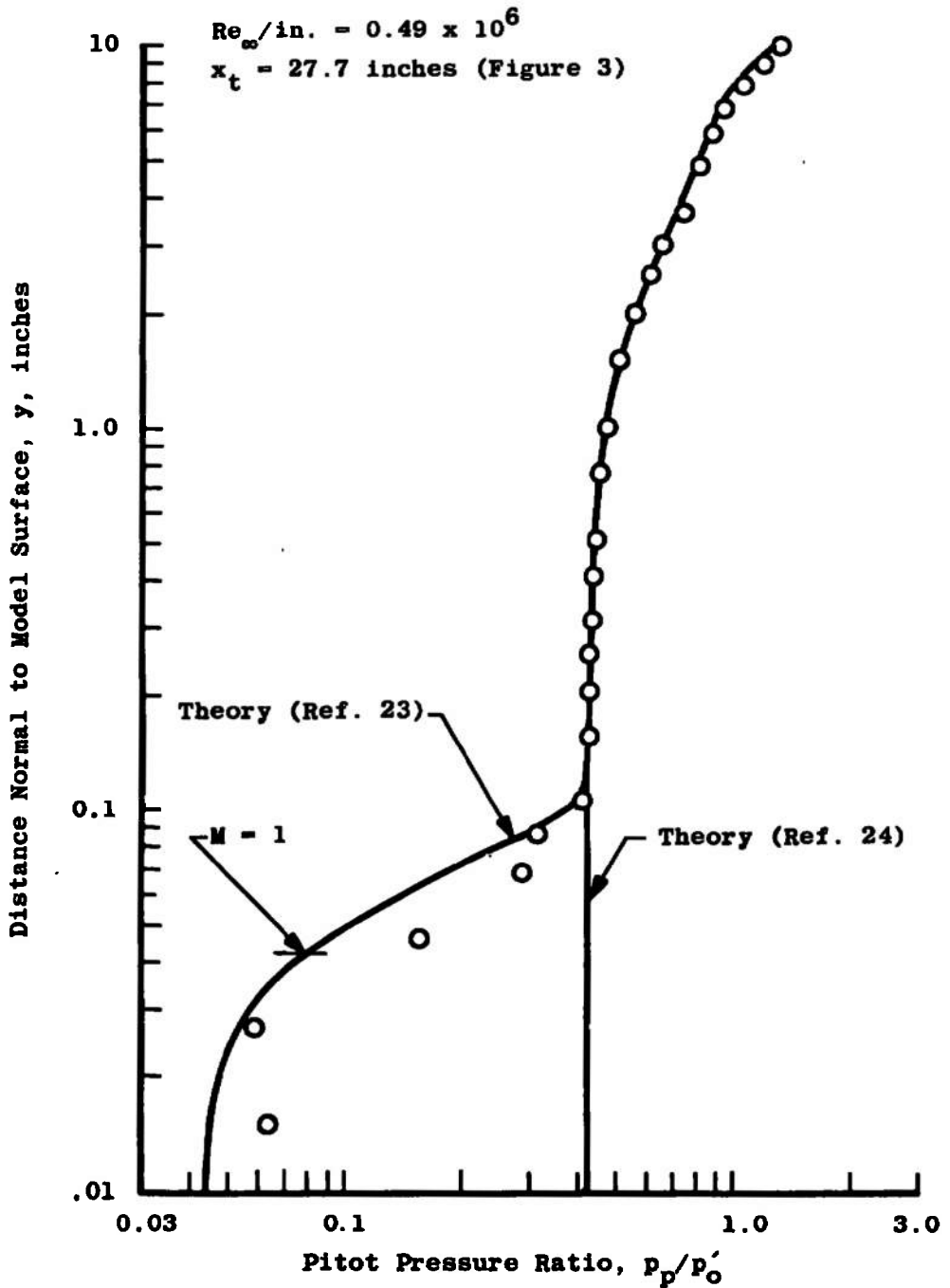
Theoretical estimates of the local "inviscid" flow characteristics for these configurations, based on the method of Inouye, Rakich, and Lomax (Ref. 24), show that the local Mach number over the cylindrical body section is in the range from 2.50 to 2.75 for all three nose shapes. At these low Mach numbers the transition Reynolds number for two-dimensional flow over a hollow cylinder is shown by Potter and Whitfield (Ref. 25) to be relatively insensitive to small Mach number changes; thus, comparison of the present blunt body transition data to the transition Reynolds numbers presented in Ref. 4 for a hollow cylinder in Tunnel A at free-stream Mach number 3 seems in order. Before this comparison is made, however, it should be noted that the curved bow shock generated by blunt bodies creates an entropy layer or so-called inviscid shear layer adjacent to the body that does not exist with a sharp leading edge.

Sym	$Re_{\infty}/in. \times 10^{-6}$	$x_t, in. (Figure 3)$
○	0.50	32.2
△	0.29	36.1

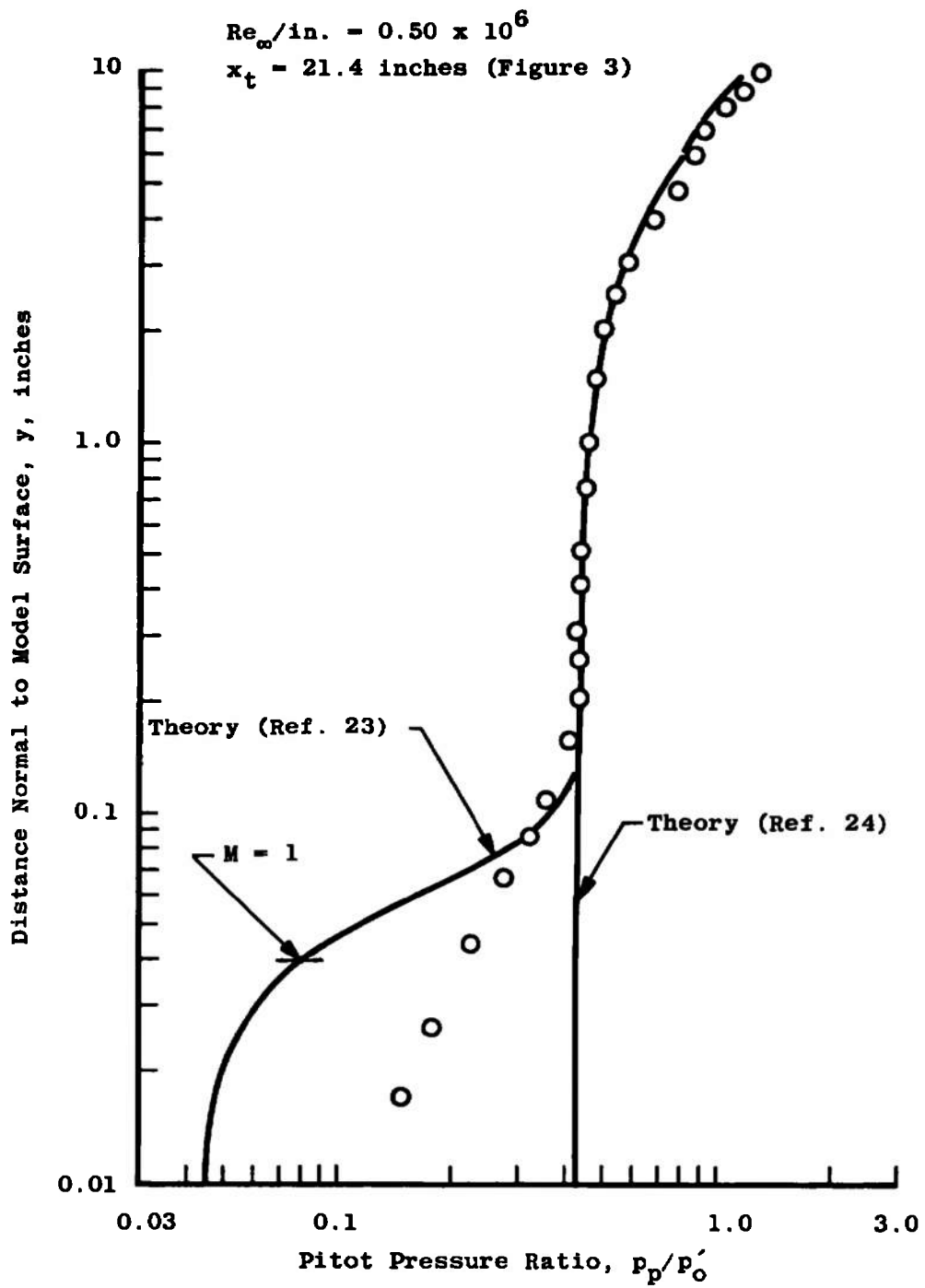


a. Sphere-Cone-Cylinder,  $x_p = 31.80$  inches

Fig. 4 Comparison of Experimental and Theoretical Pitot Pressure Profiles at  $M_{\infty} = 4$

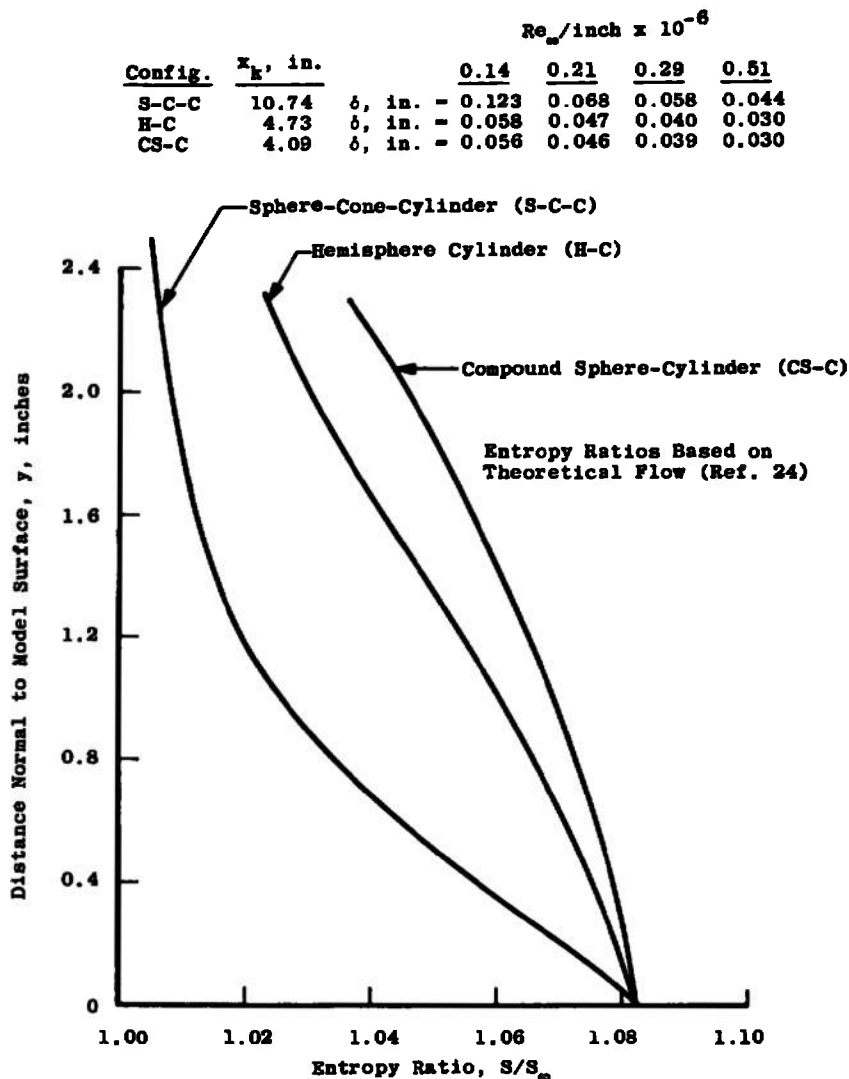


b. Hemisphere-Cylinder,  $x_p = 25.79$  inches  
 Fig. 4 Continued



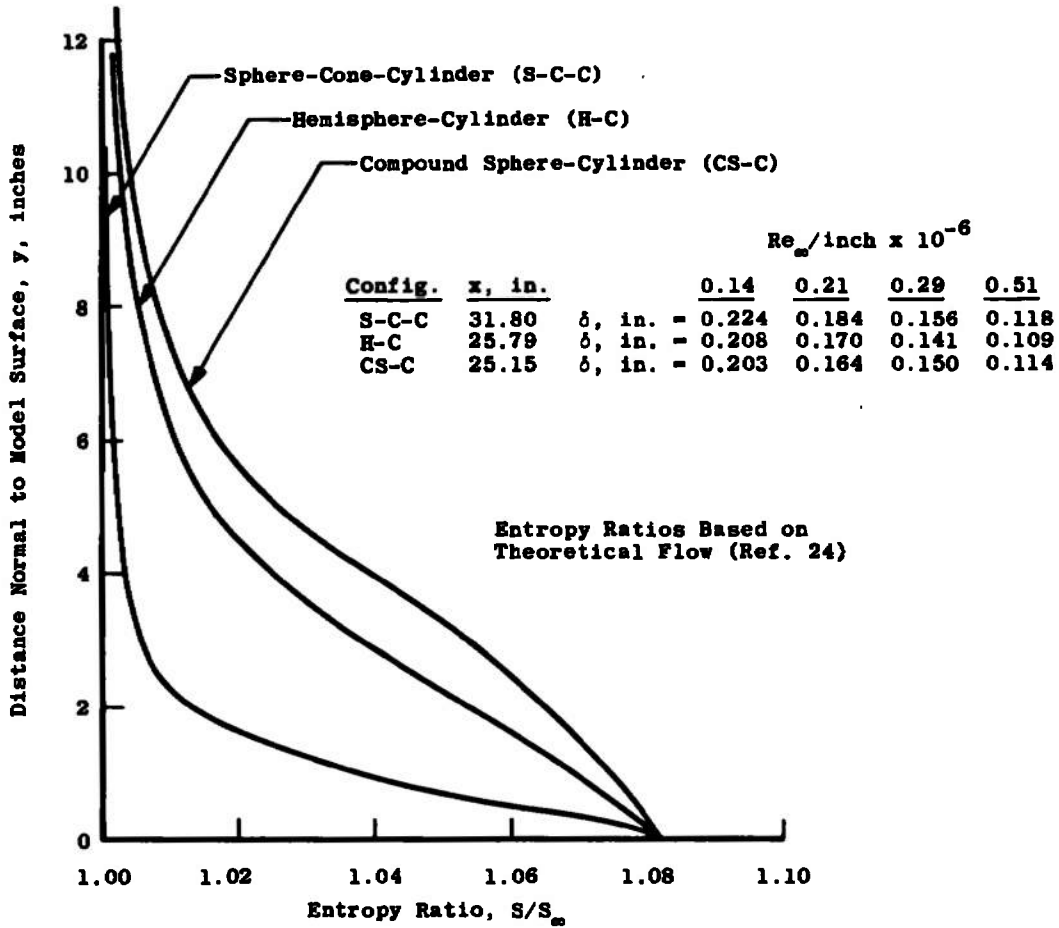
c. Compound Sphere-Cylinder,  $x_p = 25.15$  inches  
 Fig. 4 Concluded

Figure 5 shows the inviscid fluid entropy variation normal to the model surface at two axial stations for each configuration and lists the corresponding values of the boundary-layer total thickness ( $\delta$ ) based on  $\bar{u}/u_\delta = 0.995$ . It is obvious that the boundary layer constitutes only a very thin subregion of the entropy layer; thus, the entropy variations in the boundary layer are small. It was concluded by Moeckel (Ref. 26) that under these conditions and assuming identical local flow properties at the edge of the boundary layer the entropy layer has very little effect on boundary-layer development. It should be noted, however, that the thickness of the entropy layer decreases with decreasing nose radius while the total entropy change across the layer remains constant, so that the inviscid entropy gradients assume increasing importance in boundary-layer development as the nose bluntness is reduced.



a. Profiles at Boundary-Layer Trip ( $x_k$ )

Fig. 5 Entropy Variation Normal to Model Surface at  $M_\infty = 4$



b. Downstream Profiles (x<sub>k</sub> + 21.06)  
Fig. 5 Concluded

The decrease in the local unit Reynolds numbers resulting from the strong bow shock wave produced by the blunt noses of the present investigation is obvious in the comparison of transition Reynolds numbers presented in Fig. 6, since the hollow cylinder was tested over approximately the same range of free-stream unit Reynolds numbers as the present configurations. In spite of the approximate factor of four decrease in the local unit Reynolds numbers of the blunt bodies, the transition Reynolds numbers are of roughly the same order as for the relatively sharp hollow cylinder. Noting that the transition Reynolds number is the product of the local unit Reynolds number and the wetted surface distance to boundary-layer transition  $[Re_{\delta x_t} = (Re_{\delta}/in.)x_t]$ , this shows that at any given test condition transition is further downstream on the present blunt bodies than on the comparatively sharp leading-edge hollow cylinder model. Note, however, that the present data indicate a reversal in this

trend in that increasing the nose bluntness at a constant local unit Reynolds number produced a consistent reduction in the transition Reynolds number and thus an upstream movement of boundary-layer transition.

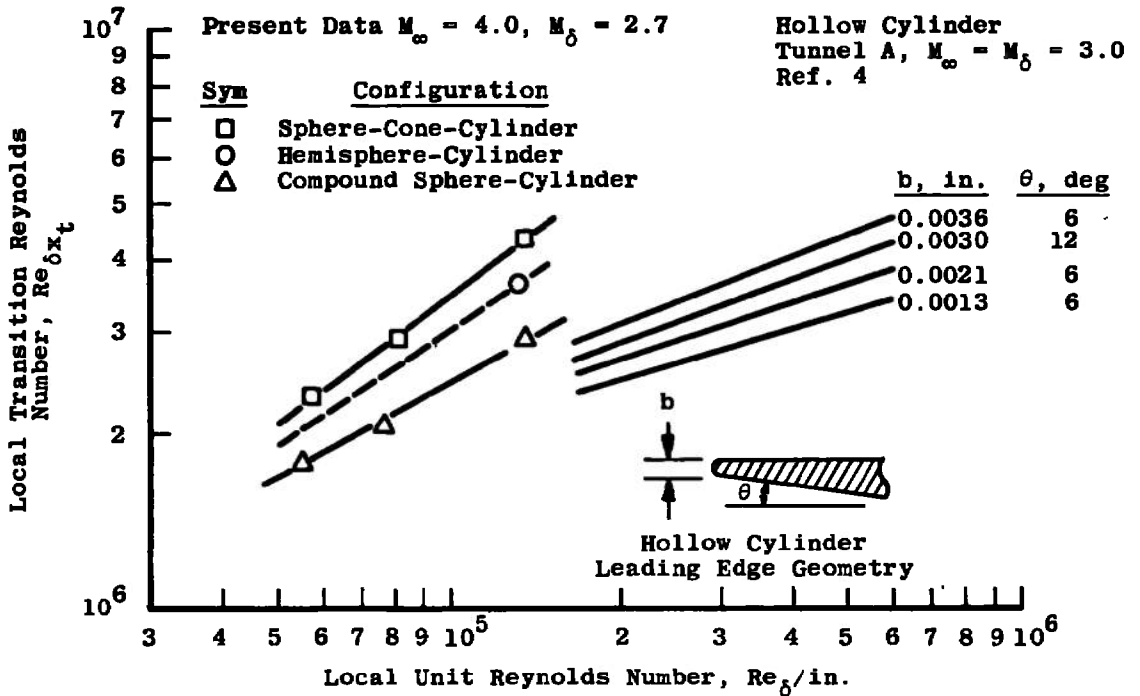
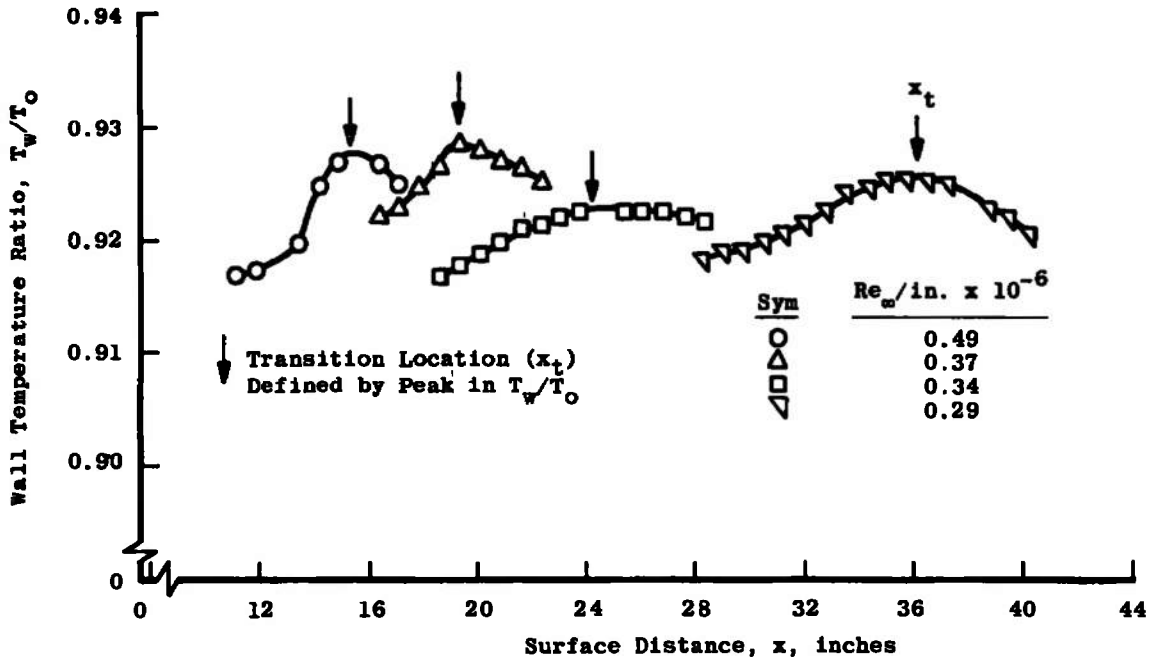
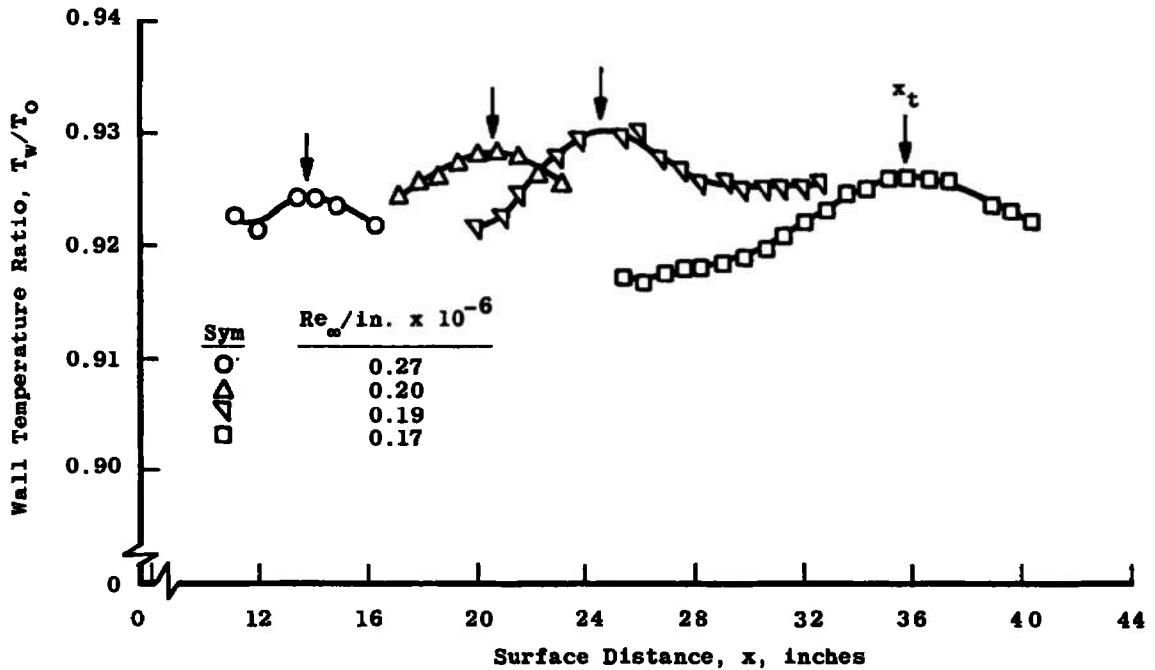


Fig. 6 Natural Transition Reynolds Number at  $M_\infty = 4$

Representative surface temperature distributions obtained with boundary-layer trips are shown in Fig. 7, with the peak temperature again being defined as representing the location of boundary-layer transition. The movement of the natural and induced transition location with free-stream unit Reynolds number is illustrated in Fig. 8, and the same data are presented as a function of the local unit Reynolds number in Fig. 9. As the unit Reynolds number is increased and the trip becomes effective, boundary-layer transition is shown to behave in a manner very similar to the two-dimensional case in that there is an abrupt deviation from the natural transition location and rapid upstream movement of transition until it reaches a point somewhat downstream of the trip. Further increases in the unit Reynolds number seem to produce a very gradual movement of transition toward the trip; however, none of the data indicated that transition had reached the trip.

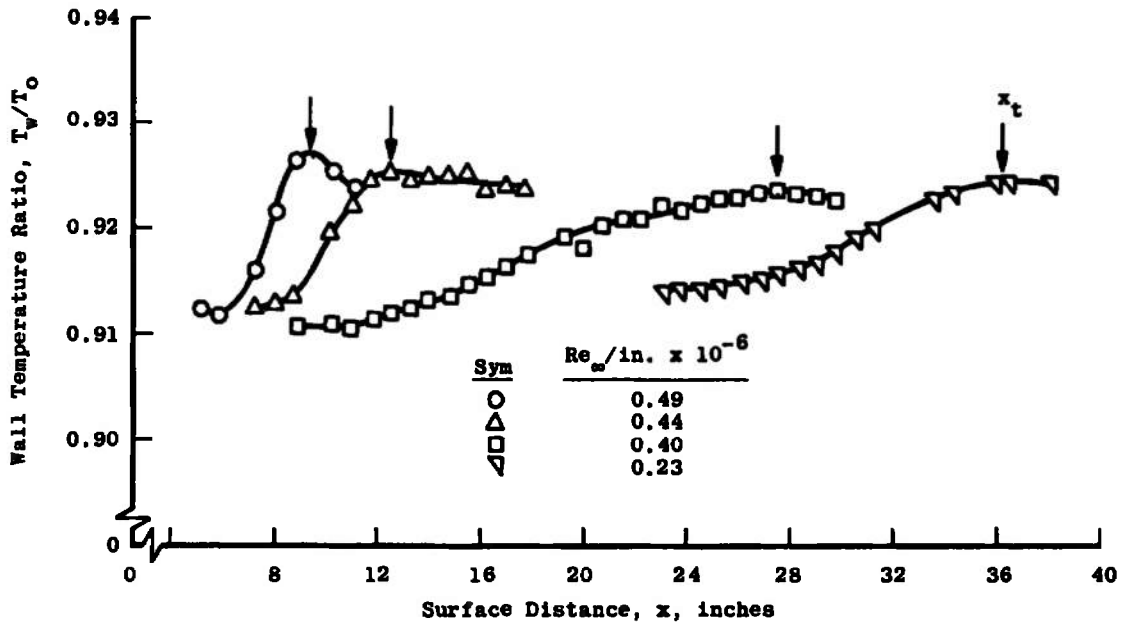


a. Sphere-Cone-Cylinder,  $k = 0.025$  inches

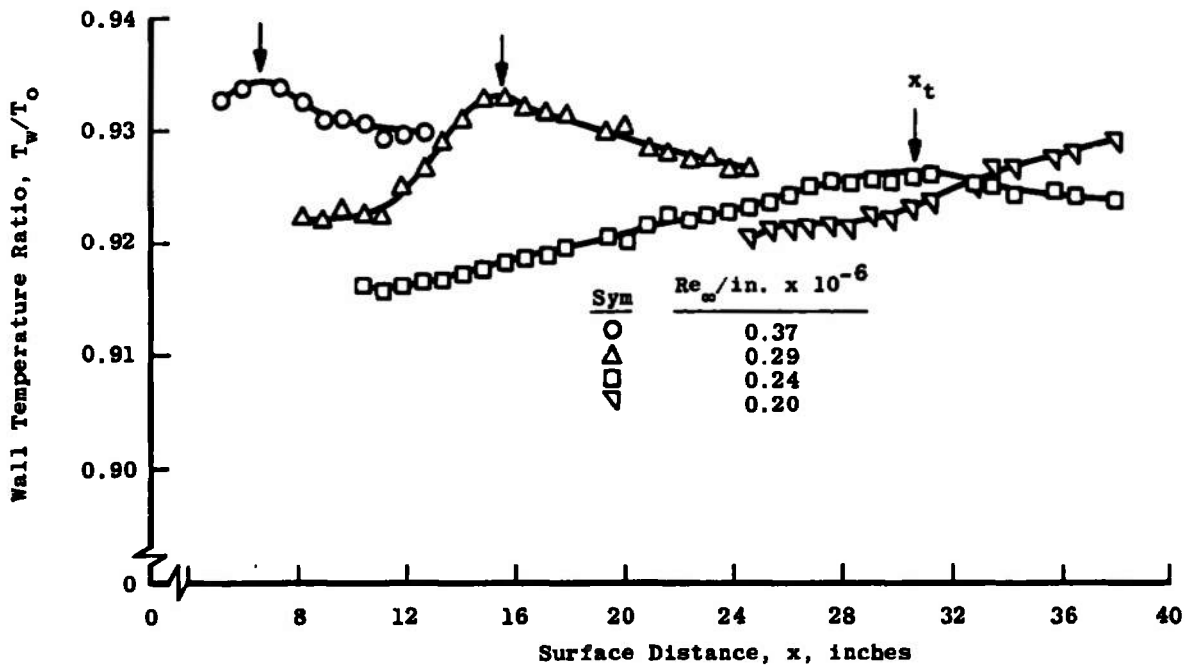


b. Sphere-Cone-Cylinder,  $k = 0.046$  inches

Fig. 7 Surface Temperature Distributions with Induced Transition at  $M_\infty = 4$

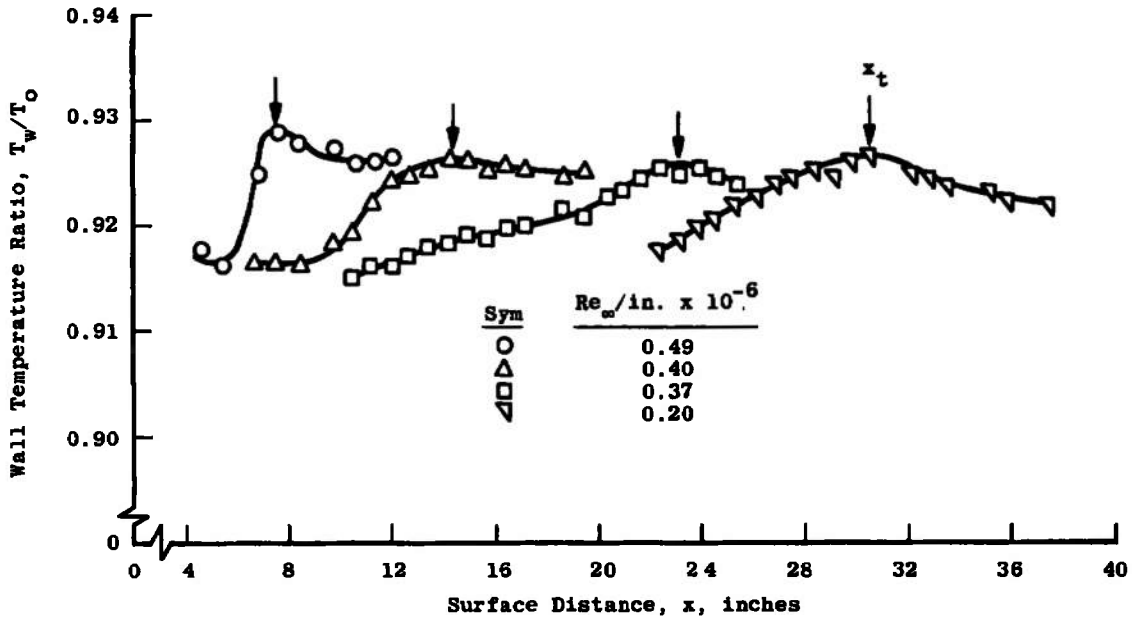


c. Hemisphere-Cylinder,  $k = 0.015$  inches

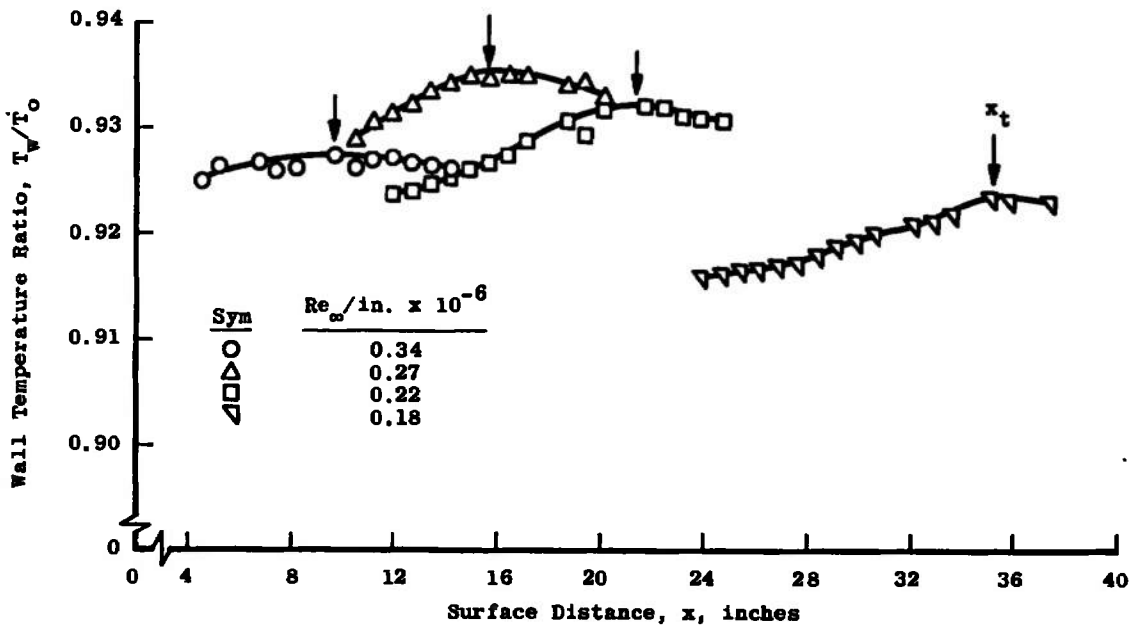


d. Hemisphere-Cylinder,  $k = 0.025$  inches

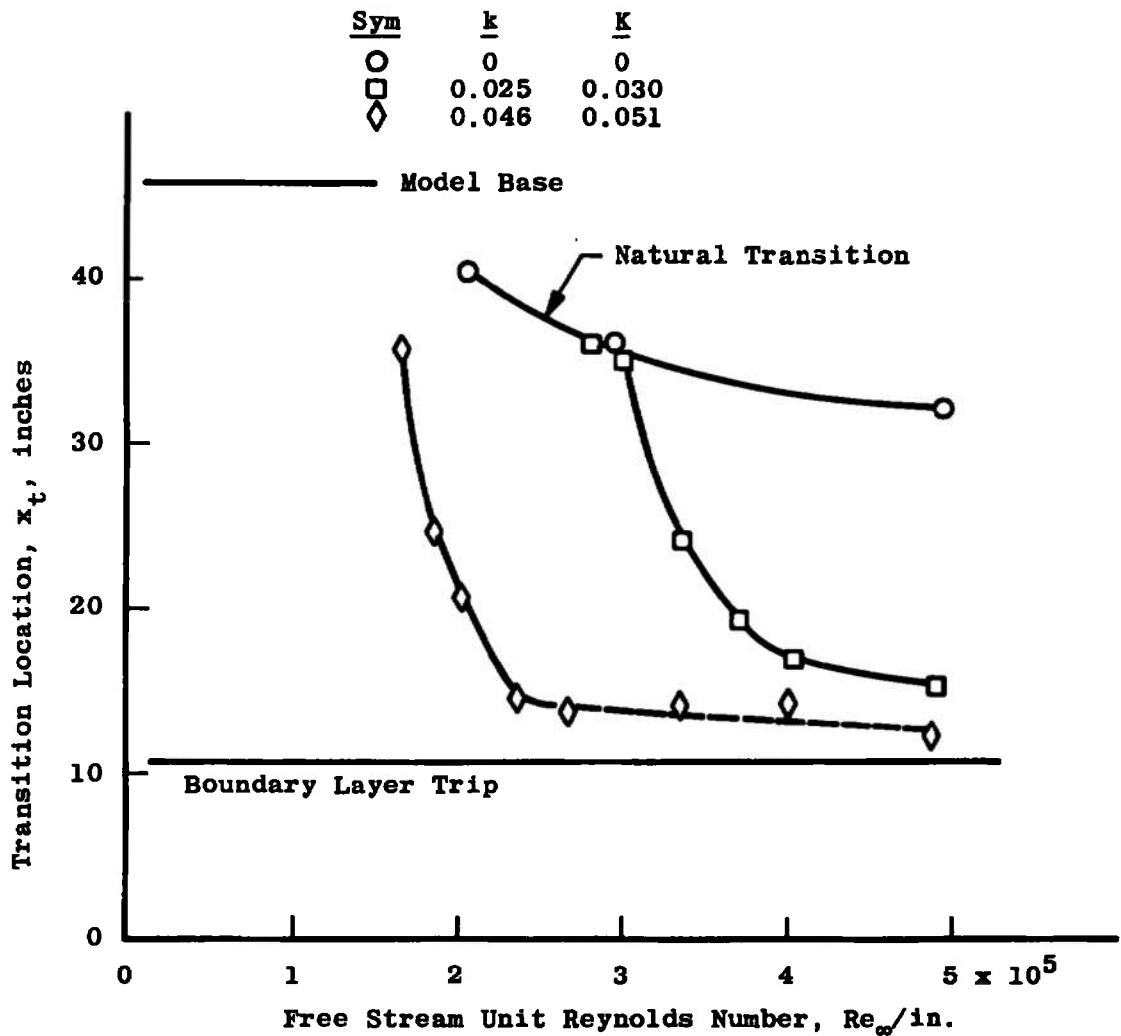
Fig. 7 Continued



e. Compound Sphere-Cylinder,  $k = 0.015$  inches

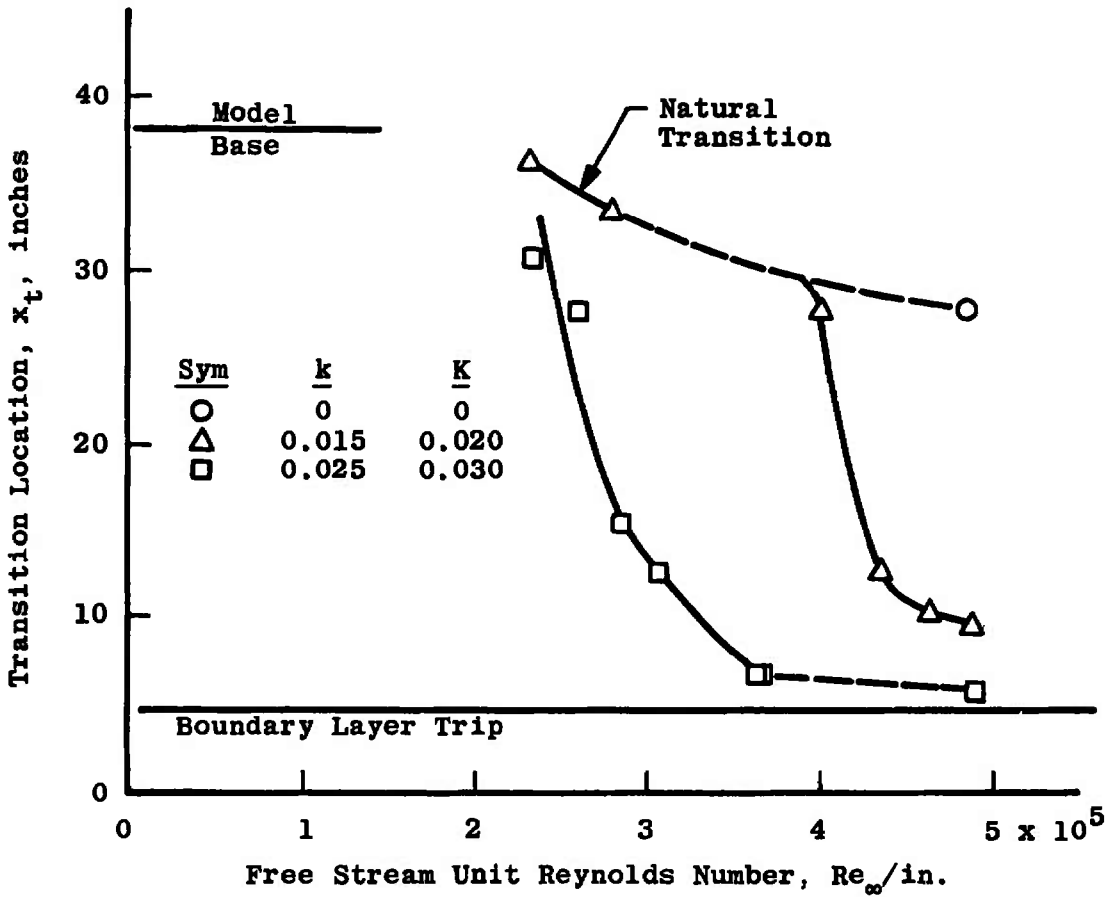


f. Compound Sphere-Cylinder,  $k = 0.025$  inches  
 Fig. 7 Concluded

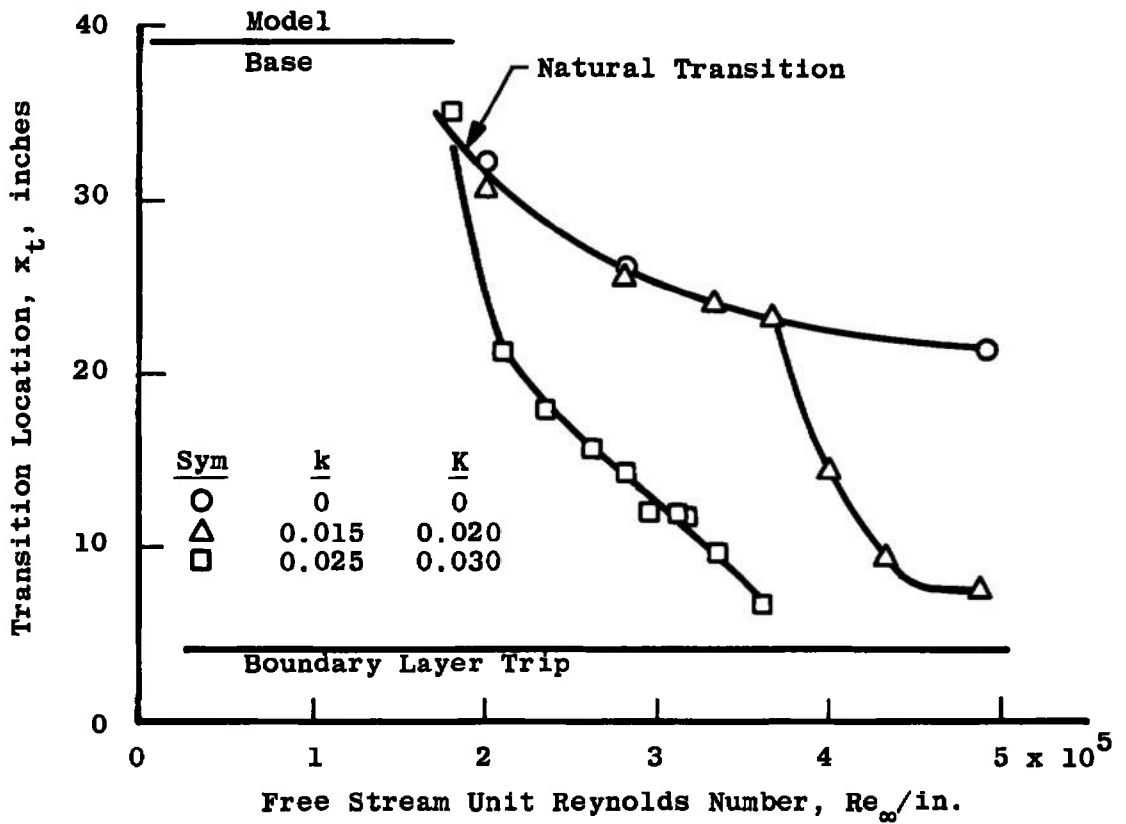


a. Sphere-Cone-Cylinder

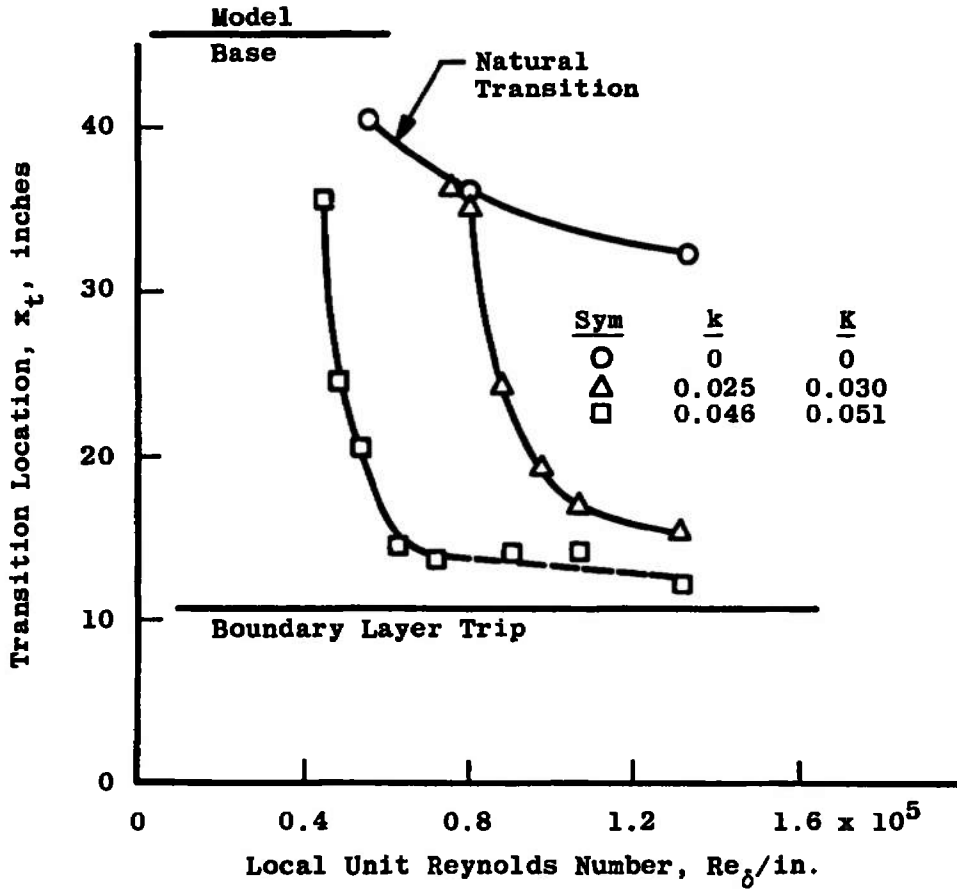
Fig. 8 Variation of Boundary Layer Transition with Free-Stream Unit Reynolds Number,  $M_\infty = 4$



b. Hemisphere-Cylinder  
Fig. 8 Continued

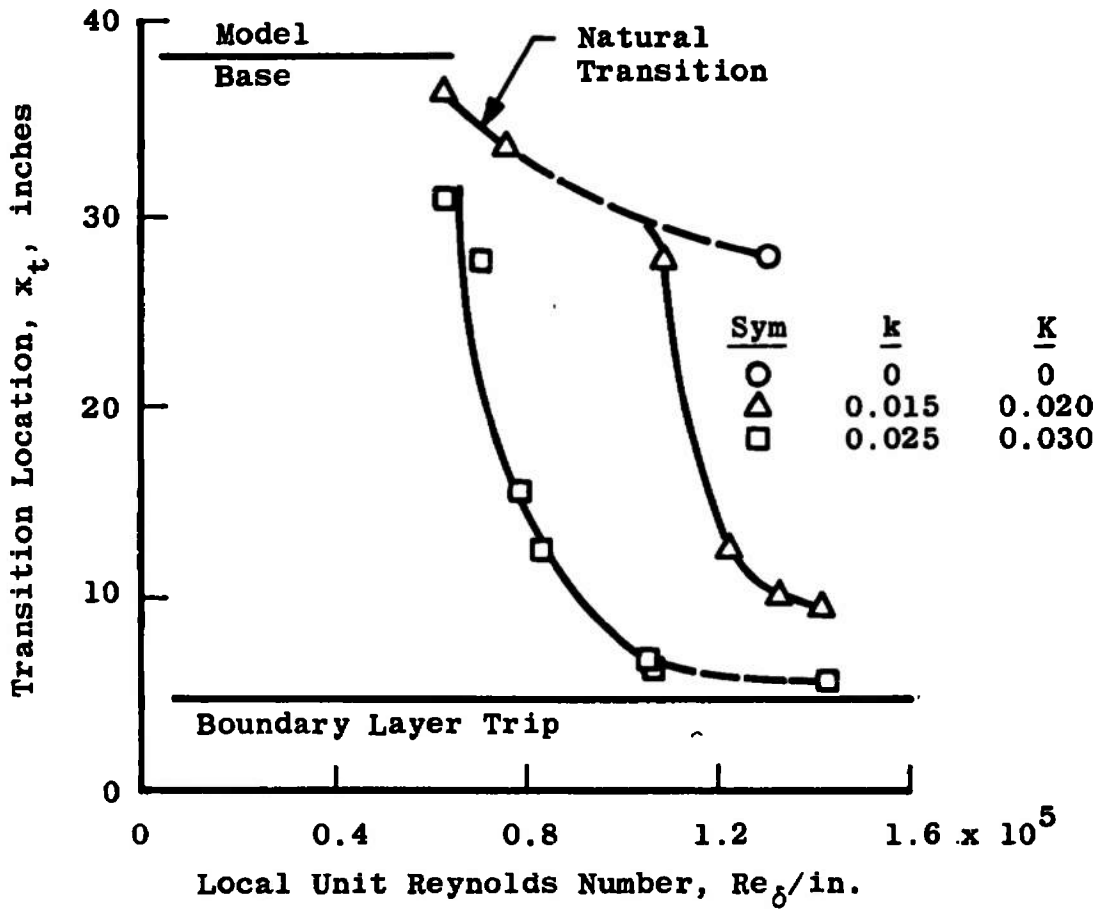


c. Compound Sphere-Cylinder  
Fig. 8 Concluded

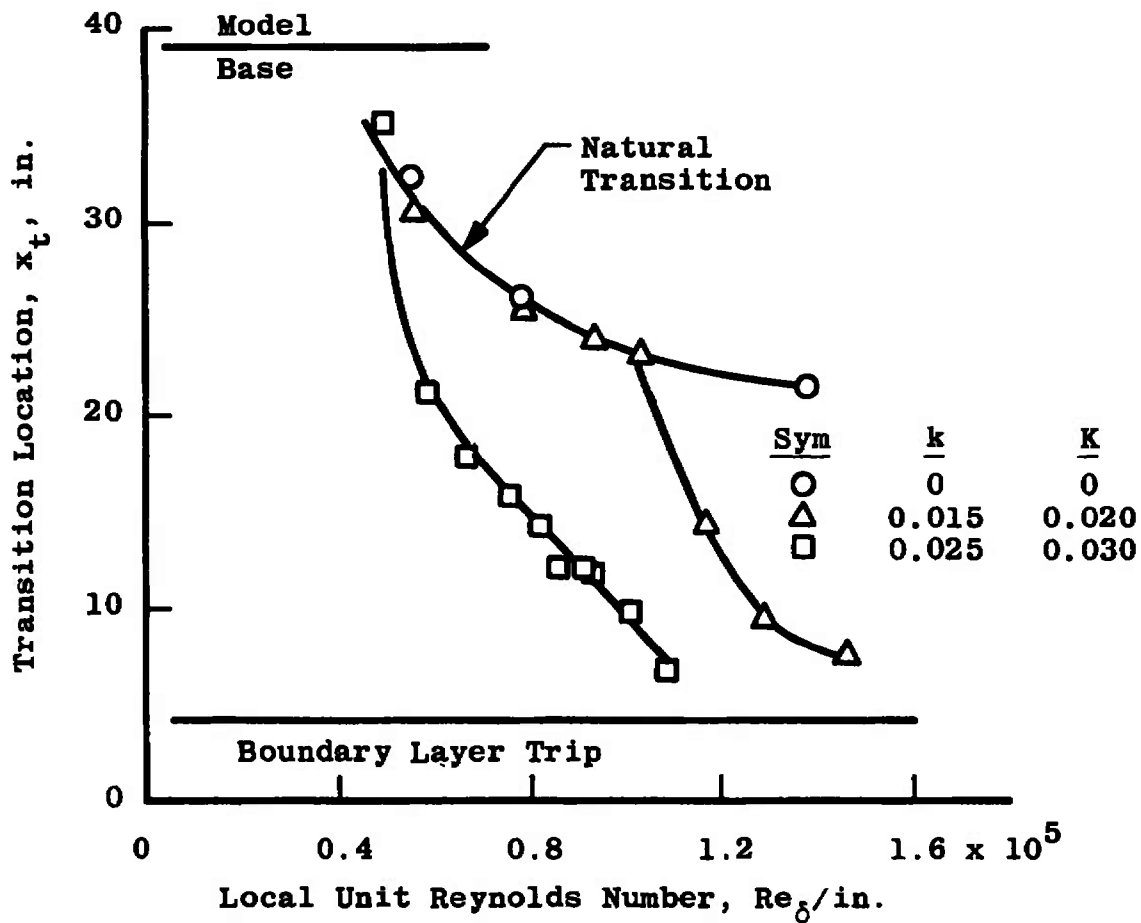


a. Sphere-Cone-Cylinder

Fig. 9 Variation of Boundary-Layer Transition with Local Unit Reynolds Number,  $M_\infty = 4$



b. Hemisphere-Cylinder  
Fig. 9 Continued



c. Compound Sphere-Cylinder  
Fig. 9 Concluded

The movement of induced boundary-layer transition from the natural transition location toward the trip is compared in Fig. 10 to the correlation proposed by Potter and Whitfield (Ref. 7) for the zero pressure gradient case of flow over a body with a sharp leading edge. The present data fall within or very near the band of data presented in Ref. 7, although it may be noted that the trend of the present data does not, in general, follow the suggested correlation curve. Nevertheless, the agreement of the data with the correlation is adequate to justify its use for obtaining at least a first approximation to the trip sizes required for very blunt bodies. A note of caution must be included regarding the validity of this or any two-dimensional correlation for bodies less blunt than those of the present investigation. The inviscid entropy layer discussed earlier may be a significant factor in the application of two-dimensional trip sizing techniques to such configurations. The very blunt noses of the present investigation produce thick entropy layers which are not believed to significantly affect either natural or induced boundary-layer transition, aside from the reduction in local Mach and unit Reynolds numbers; thus the two-dimensional techniques would be expected to be applicable. Conversely a slightly blunted body has a thin entropy layer with proportionally larger entropy gradients which must alter the boundary layer. Under these circumstances the two-dimensional techniques may not be applicable since they do not in any way account for the complicated flow resulting from absorption of the entropy layer by the boundary layer.

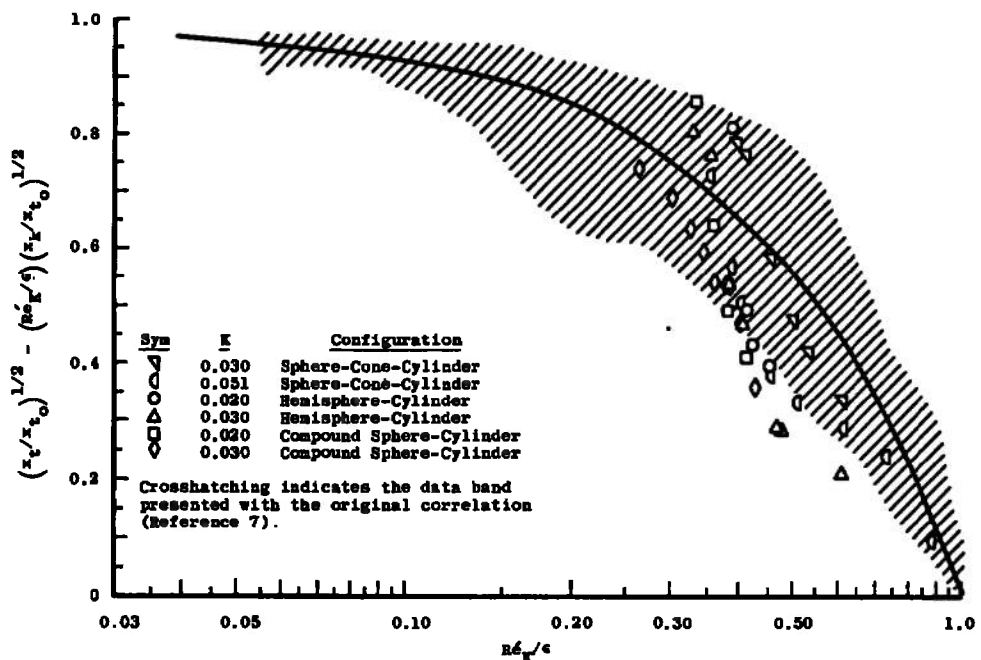


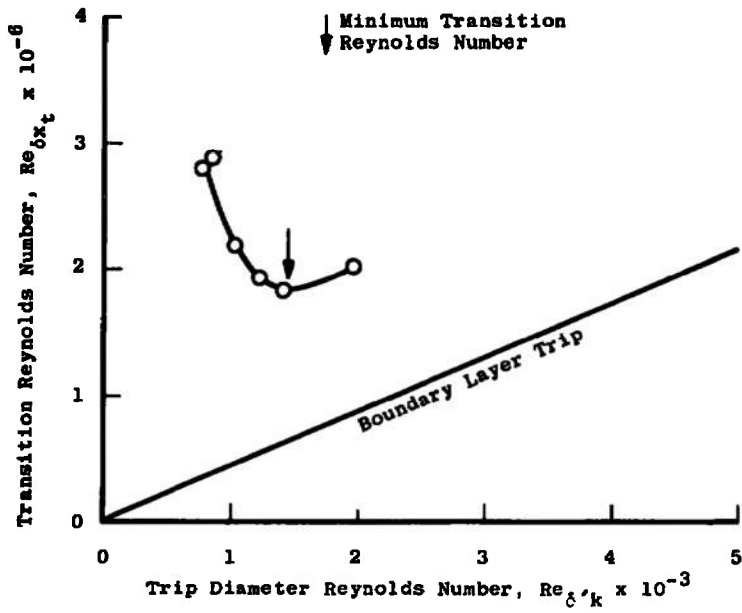
Fig. 10 Comparison of the Present Blunt Body Results at  $M_\infty = 4$  with the Potter and Whitfield Zero Pressure Gradient Correlation

One fact noted by Potter and Whitfield (Ref. 7) regarding the application of their trip sizing technique at high free-stream Mach numbers that may be even more important in blunt body applications is that moving transition to the trip will require a very large trip diameter relative to the local boundary-layer thickness. A large trip will, of course, increase the likelihood of encountering undesirable secondary stream disturbances. Selection of a downstream limit for the location of boundary-layer transition that is compatible with both the test objectives and the test conditions is considered more practical than bringing transition to the trip. Using this criteria in applying the Potter and Whitfield technique will in most cases significantly reduce the estimated trip sizes since the required trip diameter generally decreases very rapidly with the initial increase in the distance between the trip and boundary-layer transition ( $x_t - x_k$ ).

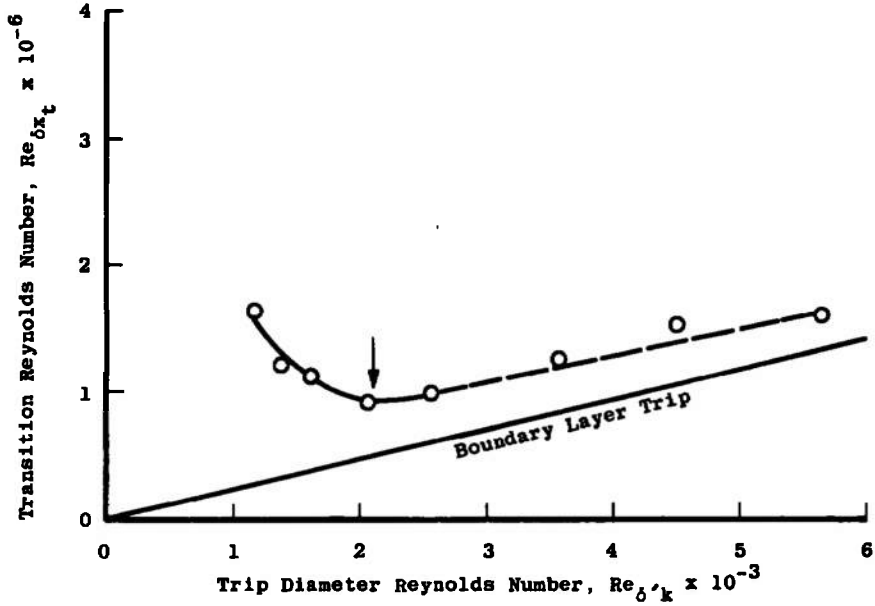
Van Driest and Blummer (Ref. 13) have proposed a trip sizing technique applicable to blunt bodies with equilibrium wall temperatures. The method proposes to define the trip size that will yield the minimum transition Reynolds number which occurs in the region where induced transition ceases its rapid upstream movement and begins gradually approaching the trip. The method was developed from data obtained on a sphere at Mach number 2 but also showed good agreement with data obtained on a sharp cone at surface Mach numbers from near 0 to 3.67. The correlation curve is given by the equation:

$$\frac{Re\delta^*k}{1 + \frac{\gamma-1}{2} M\delta^{*2}} \left( \frac{k/\delta^*k}{1 + 700 \frac{k}{D}} \right)^2 \left[ 1 - 0.222 \left( \frac{k/\delta^*k}{1 + 700 \frac{k}{D}} \right) + 0.009 \left( \frac{k/\delta^*k}{1 + 700 \frac{k}{D}} \right)^2 + 0.001 \left( \frac{k/\delta^*k}{1 + 700 \frac{k}{D}} \right)^3 \right] = 807 \quad (1)$$

The present data are shown in Fig. 11 in the form used by van Driest and Blummer (Ref. 13) to obtain the minimum transition Reynolds numbers. The estimated minimums, indicated by arrows in Fig. 11, were used in conjunction with the theoretical boundary-layer characteristics to define the displacement thickness Reynolds numbers for comparison with the van Driest and Blummer correlation in Fig. 12. The present data obviously do not match the correlation. However, examination of the Mach number 2 sphere data and the present results revealed that a modification of the empirical van Driest and Blummer correlation would provide a relationship applicable to both sets of data.

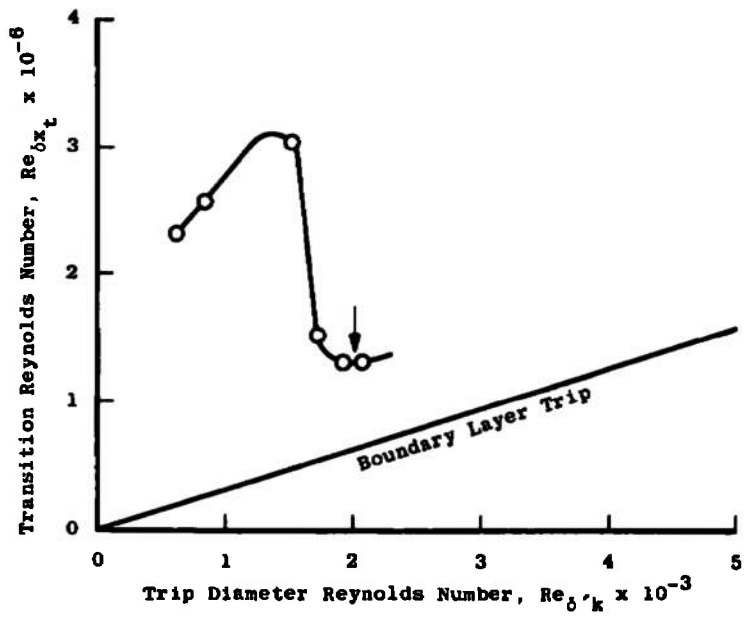


a. Sphere-Cone-Cylinder,  $k = 0.025$  inches

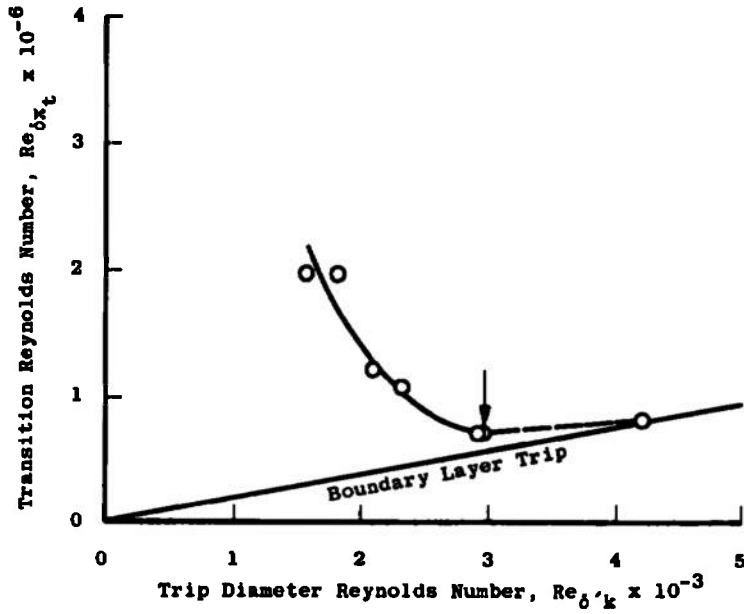


b. Sphere-Cone-Cylinder,  $k = 0.046$  inches

Fig. 11 Variation of the Transition Reynolds Number with Trip Diameter Reynolds Number

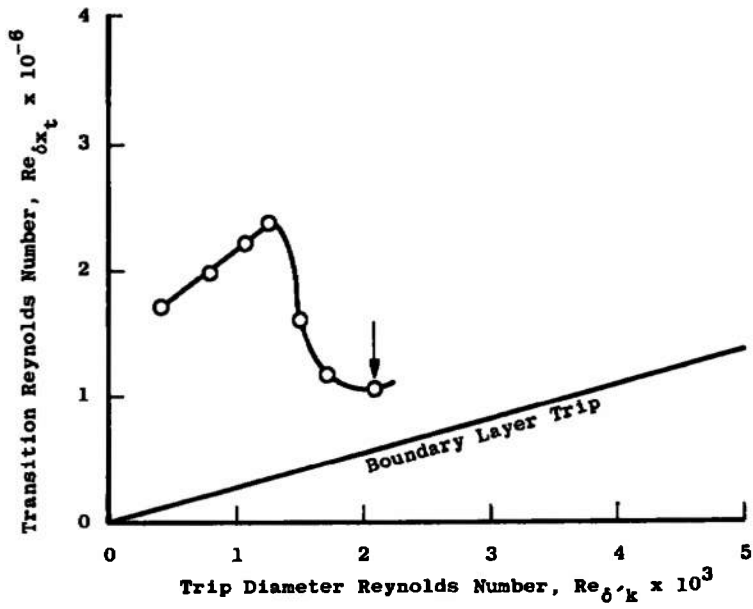


c. Hemisphere-Cylinder,  $k = 0.015$  inches

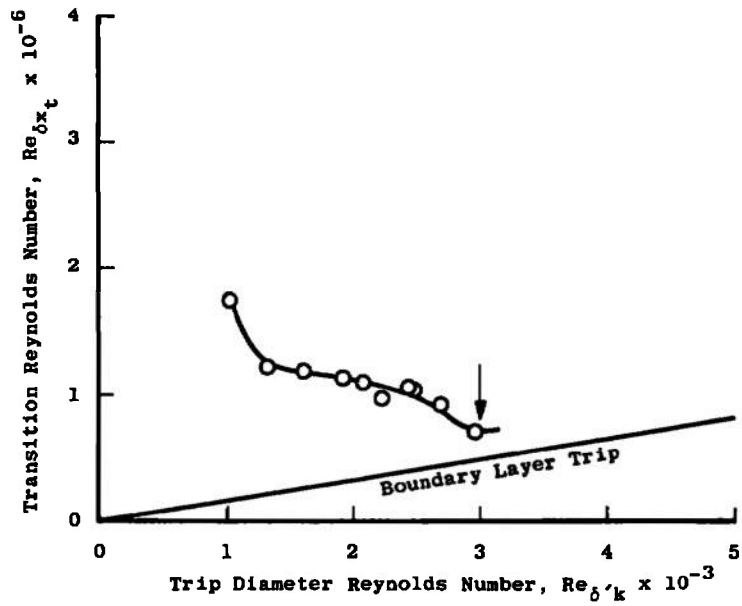


d. Hemisphere-Cylinder,  $k = 0.025$  inches

Fig. 11 Continued



e. Compound Sphere-Cylinder,  $k = 0.015$  inches



f. Compound Sphere-Cylinder,  $k = 0.025$  inches

Fig. 11 Concluded

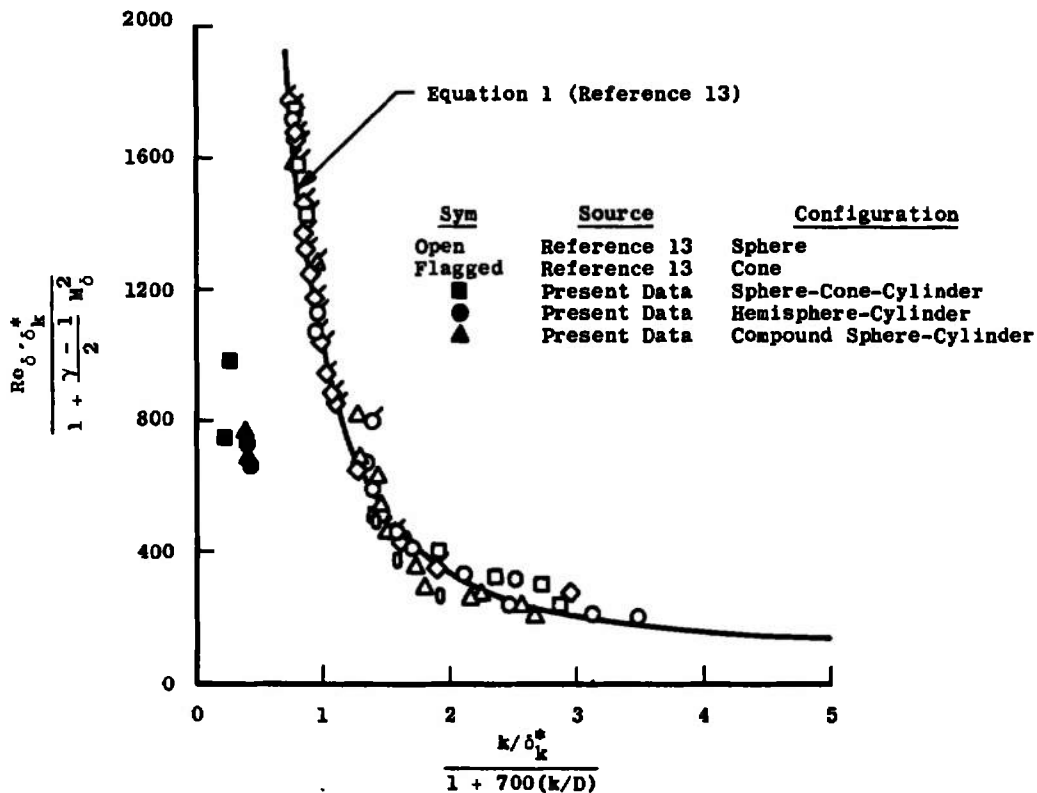


Fig. 12 Comparison of the Present Data with the Results and Correlation of van Driest and Blummer

As shown in Fig. 13, substitution of  $[17.65 + (p'_0/p_0)(M_{ch})]^2 k/D$  for  $700 k/D$  in the denominator of the abscissa provided a satisfactory correlation for the zero pressure gradient data on a sharp cone and the available blunt body data at equilibrium wall temperatures at Mach numbers 2 and 4. The correlation equation now has the form:

$$\frac{Re_{\delta^*k}}{\left(1 + \frac{\gamma-1}{2} M_\infty^2\right)} = \frac{k/\delta^*k}{f(M_\infty)} \left[ 1 - 0.222 \left(\frac{k/\delta^*k}{f(M_\infty)}\right) + 0.009 \left(\frac{k/\delta^*k}{f(M_\infty)}\right)^2 + 0.001 \left(\frac{k/\delta^*k}{f(M_\infty)}\right)^3 \right] = 807 \tag{2}$$

where

$$f(M_\infty) = 1 + [17.65 (p'_0/p_0) (M_{ch})]^2 k/D \tag{3}$$

It should be noted that the model diameter (D) has been assumed to be infinite for constant pressure flow over a sharp cone in order to be compatible with zero pressure gradient flow over a flat plate. Since the denominator of the abscissa  $[f(M_\infty)]$  approaches one as D approaches infinity, the change in the correlation does not affect the sharp cone data and could therefore be thought of as accounting for free-stream Mach number effects on trip effectiveness for blunt bodies. This would give

credence to the selection of the inviscid local model surface stagnation pressure loss and a characteristic surface Mach number (the local Mach number at the nose-body junction was selected in this case) to modify the trip sizing correlation of van Driest and Blummer. Regardless of this and the apparent success of the modified correlation, it must be emphasized that only a limited amount of data, all obtained on very blunt configurations with equilibrium surface temperatures over a limited Mach number range, has been considered and care must be taken not to assume general applicability without experimental confirmation.

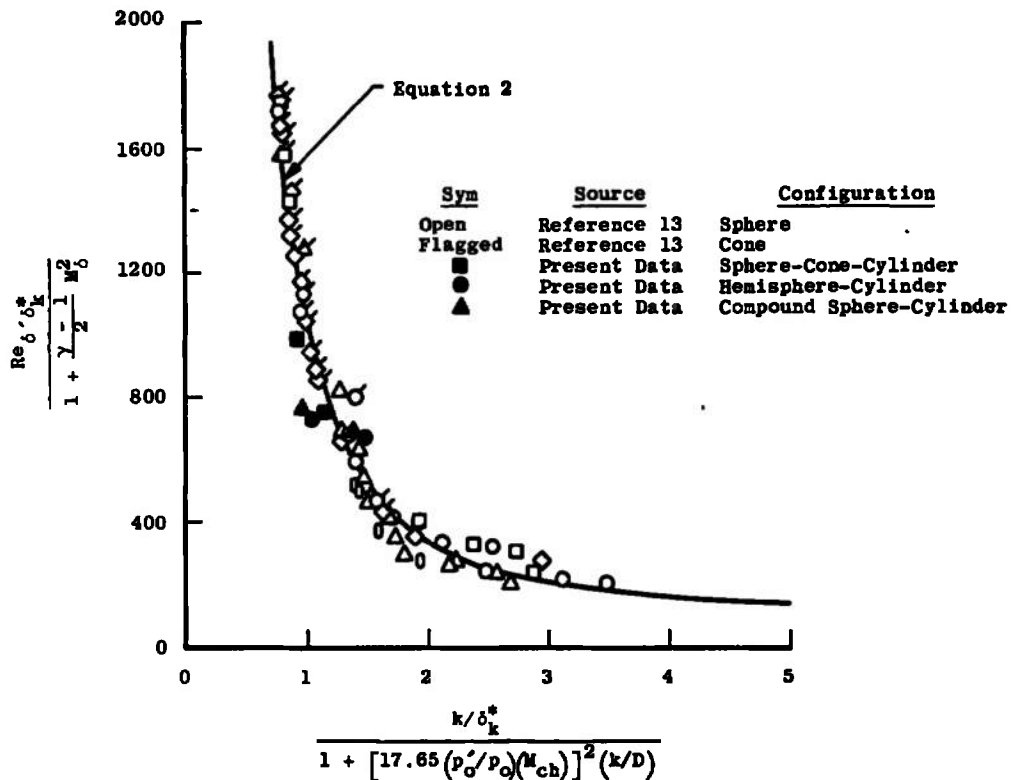


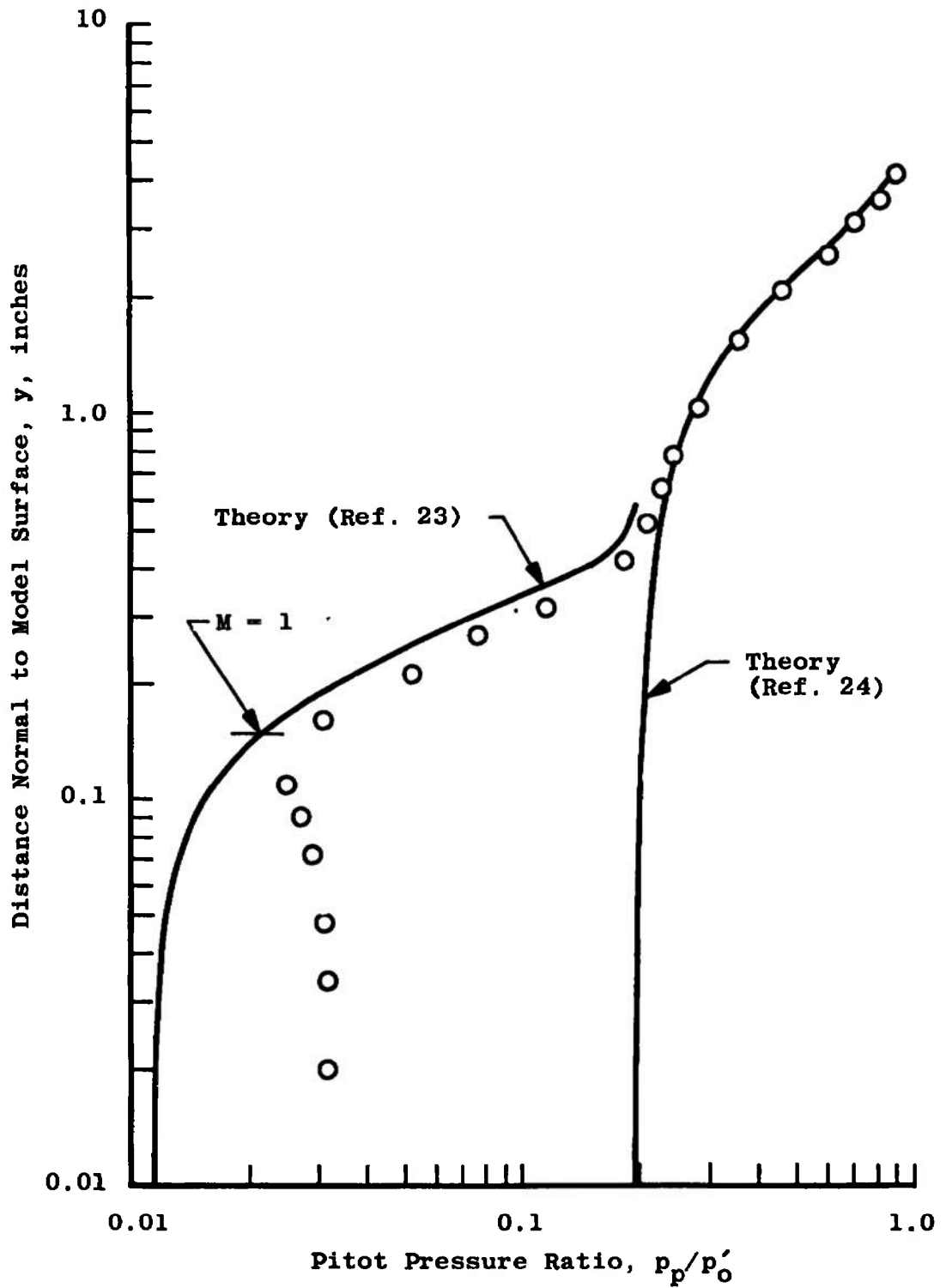
Fig. 13 Comparison of the Present Data and the Results of van Driest and Blummer with the Modified Correlation

A very difficult problem in evaluating the effectiveness of boundary-layer trips on the basis of measured pitot pressure profiles was examined by Potter and Whitfield (Ref. 20) on a relatively sharp leading-edge hollow cylinder. Although the characteristics of the boundary layer on a blunt body will be different, the same basic problem must be expected to exist. Using a y-coordinate nondimensionalized with the total boundary-layer thickness ( $\delta$ ), they compared a pitot pressure profile at a station downstream from natural transition to a profile obtained at a station considerably further upstream but also downstream of transition effected

with boundary-layer trips. The two profiles were identical throughout the outer 80 percent of the boundary layer; however, close to the model surface the pitot pressure for the induced transition case suddenly deviated toward a laminar profile at the same station obtained without boundary-layer trips. The model wall temperature distributions showed that, in spite of the turbulent characteristics of all but a thin subregion of the boundary layer, the peak wall temperature was not reached upstream of the location of natural transition. From this it must be concluded that a boundary-layer trip may produce a predominantly turbulent pitot pressure profile in the outer part of the boundary layer without causing any noticeable upstream movement of the location of fully developed turbulence in the innermost regions of the boundary layer. In view of this, the pitot pressure profile seems to be of little use in induced transition studies unless a fully developed turbulent profile is indicated. In the present data this was not the case; instead, there was the same abrupt deviation toward the laminar profile that was noted by Potter and Whitfield.

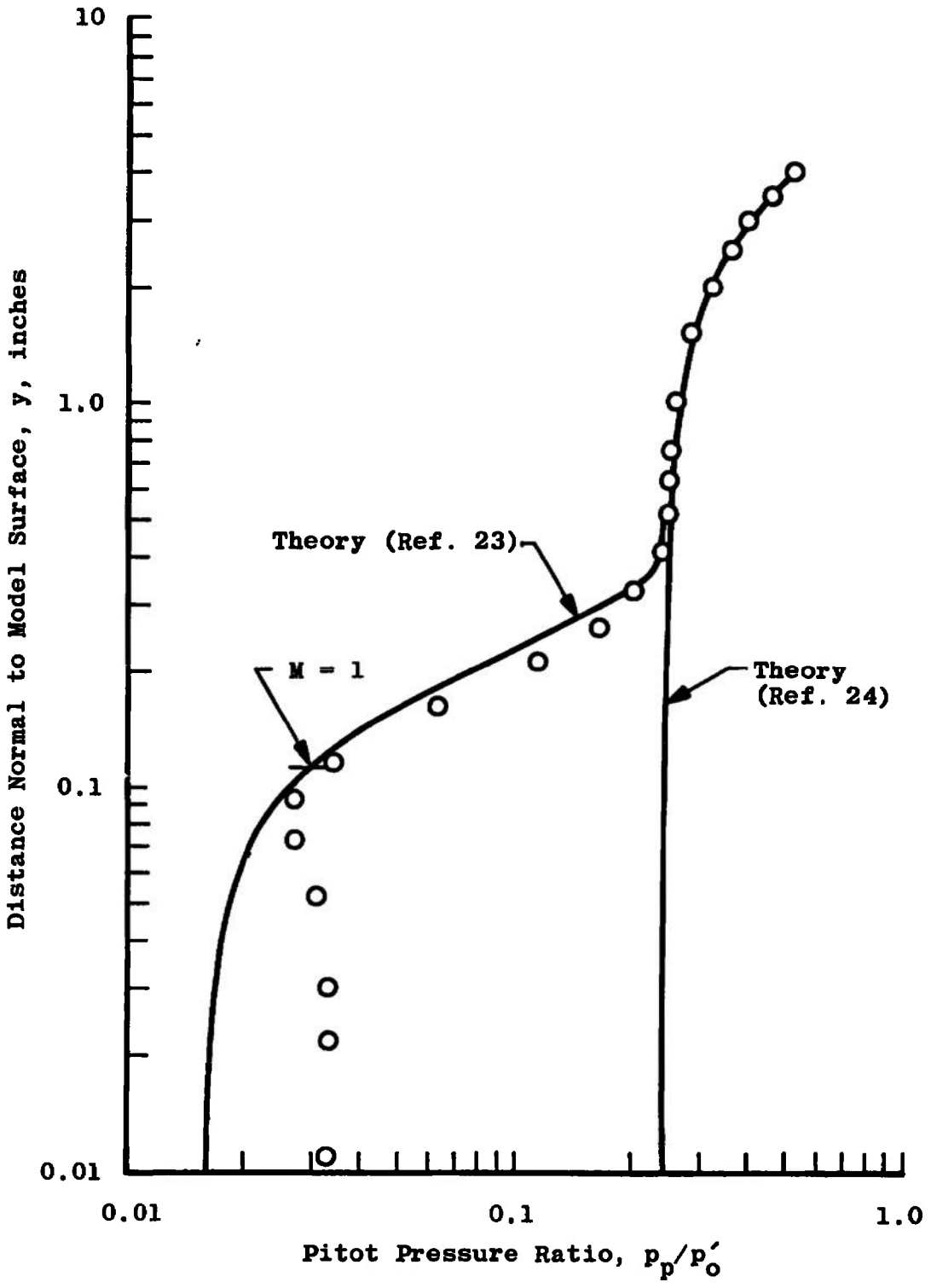
Some data obtained at Mach number 8 may be of interest, however, in spite of the difficulty in interpretation. Experimental pitot pressure profiles obtained without boundary-layer trips at a station 14 in. forward of the model base are compared in Fig. 14 to theoretical estimates for a laminar boundary layer. As previously noted, the theoretical predictions appeared to slightly overestimate the actual boundary-layer thickness, and it should also be noted that the experimental and theoretical values diverged near the model surface. This may have been caused by probe interference; that is, as the probe approached the model surface a disturbance was set up that disrupted the flow such that it no longer corresponded to the undisturbed boundary layer. No systematic investigation was undertaken to confirm that the probe was responsible for the trend of these pitot pressures measured close to the model surface. Comparison of the profiles obtained with the locations of sonic velocity (included on the figures for each pitot pressure profile) reveals that the irregularities were present only in the subsonic regions of the boundary layer. This is typical of probe interference which generally disappears in regions of supersonic flow.

The effects of boundary-layer trips on the pitot pressure profiles at various downstream stations are illustrated by comparison with theoretical profiles in Fig. 15. Immediately downstream of the trip,  $(x_p - x_k) = 2.88$  in., the primary effect was a thickening of the boundary layer, and a near linear profile characteristic of a turbulent boundary layer appeared to develop gradually as the flow progressed downstream.

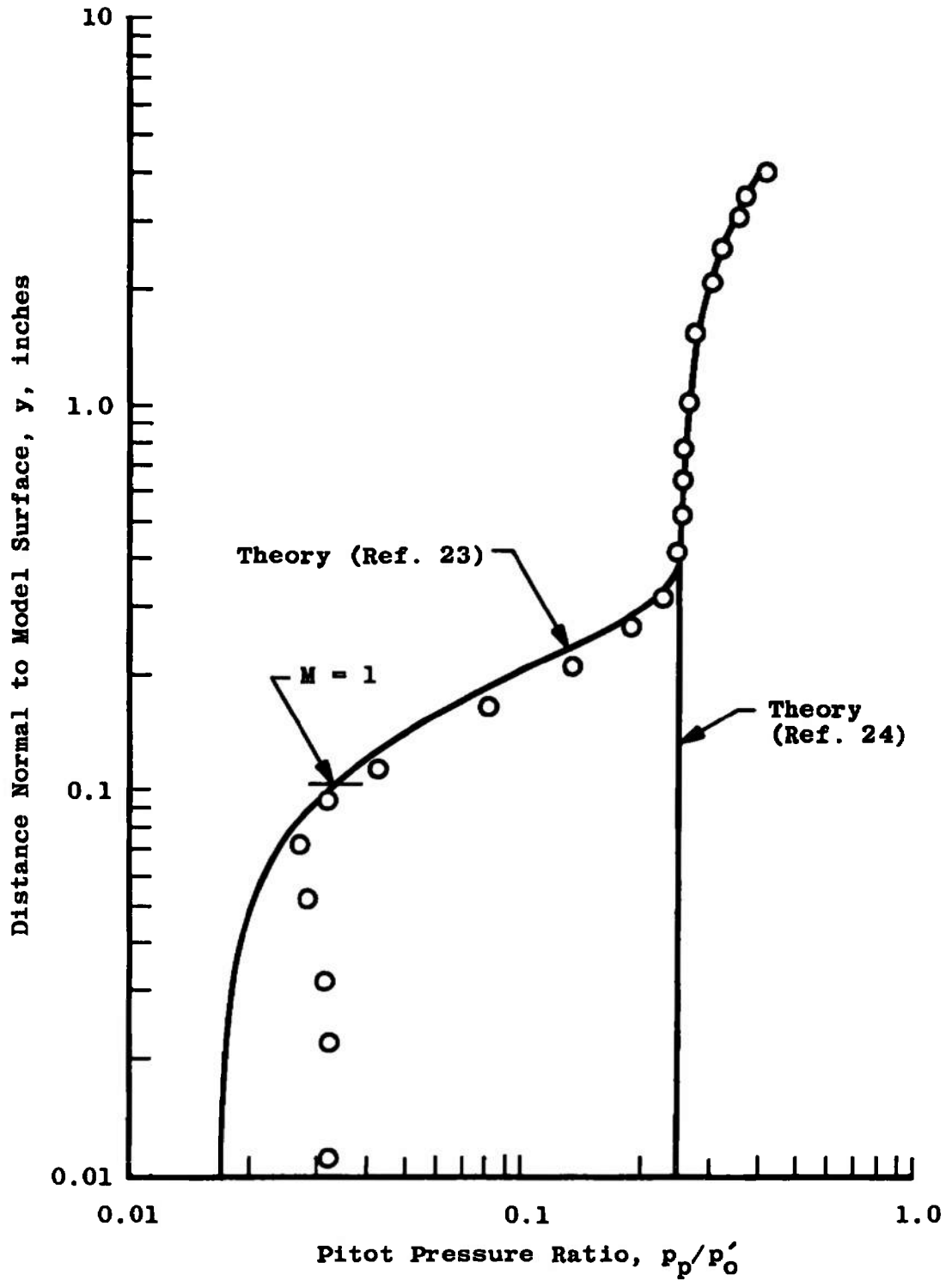


a. Sphere-Cone-Cylinder,  $x_p = 31.80$  inches

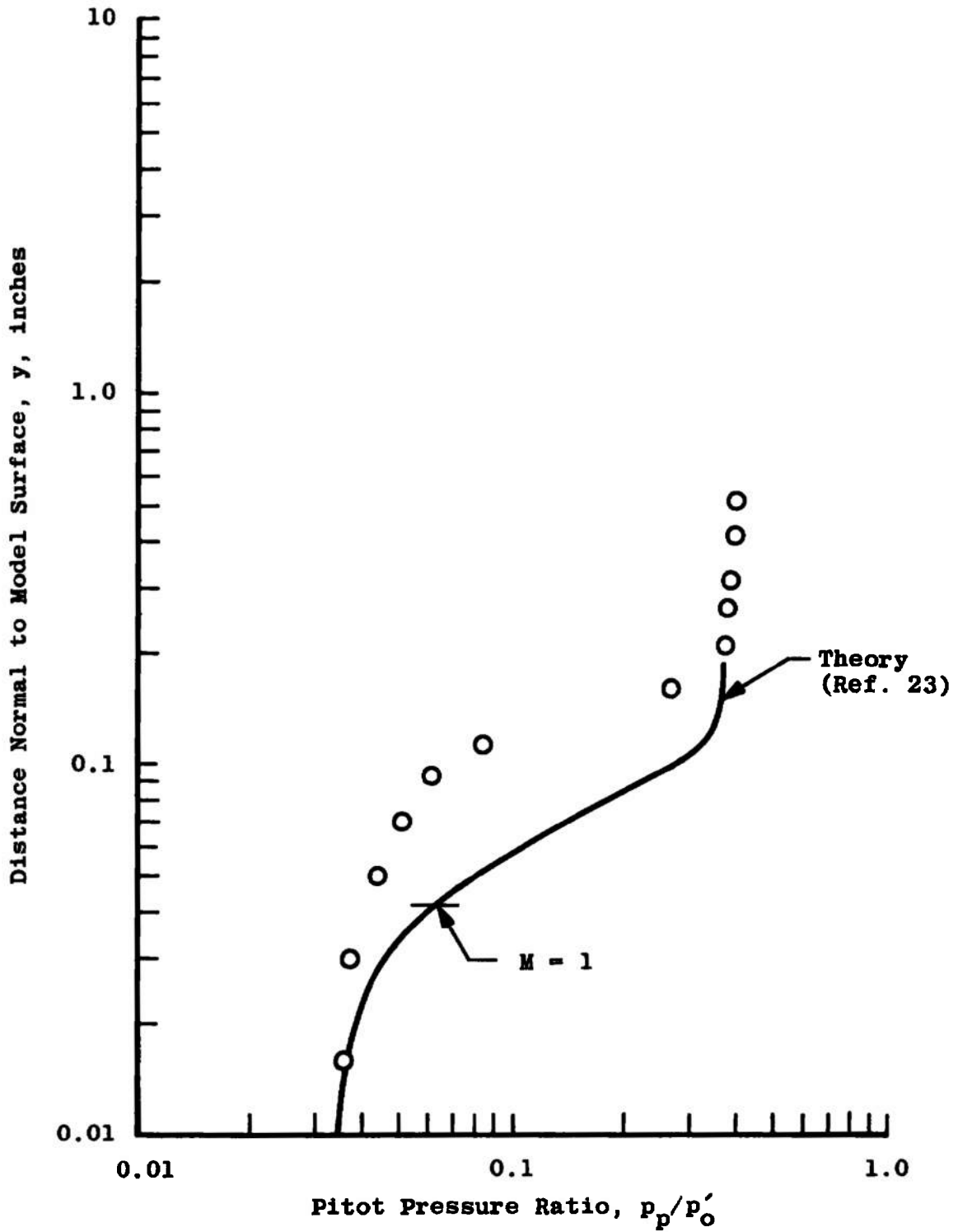
Fig. 14 Comparison of Laminar Boundary-Layer Pitot Pressure Profiles with Theoretical Estimates at  $M_\infty = 8$ ,  $Re_\infty/in. = 0.19 \times 10^6$



b. Hemisphere-Cylinder,  $x_p = 25.79$  inches  
 Fig. 14 Continued

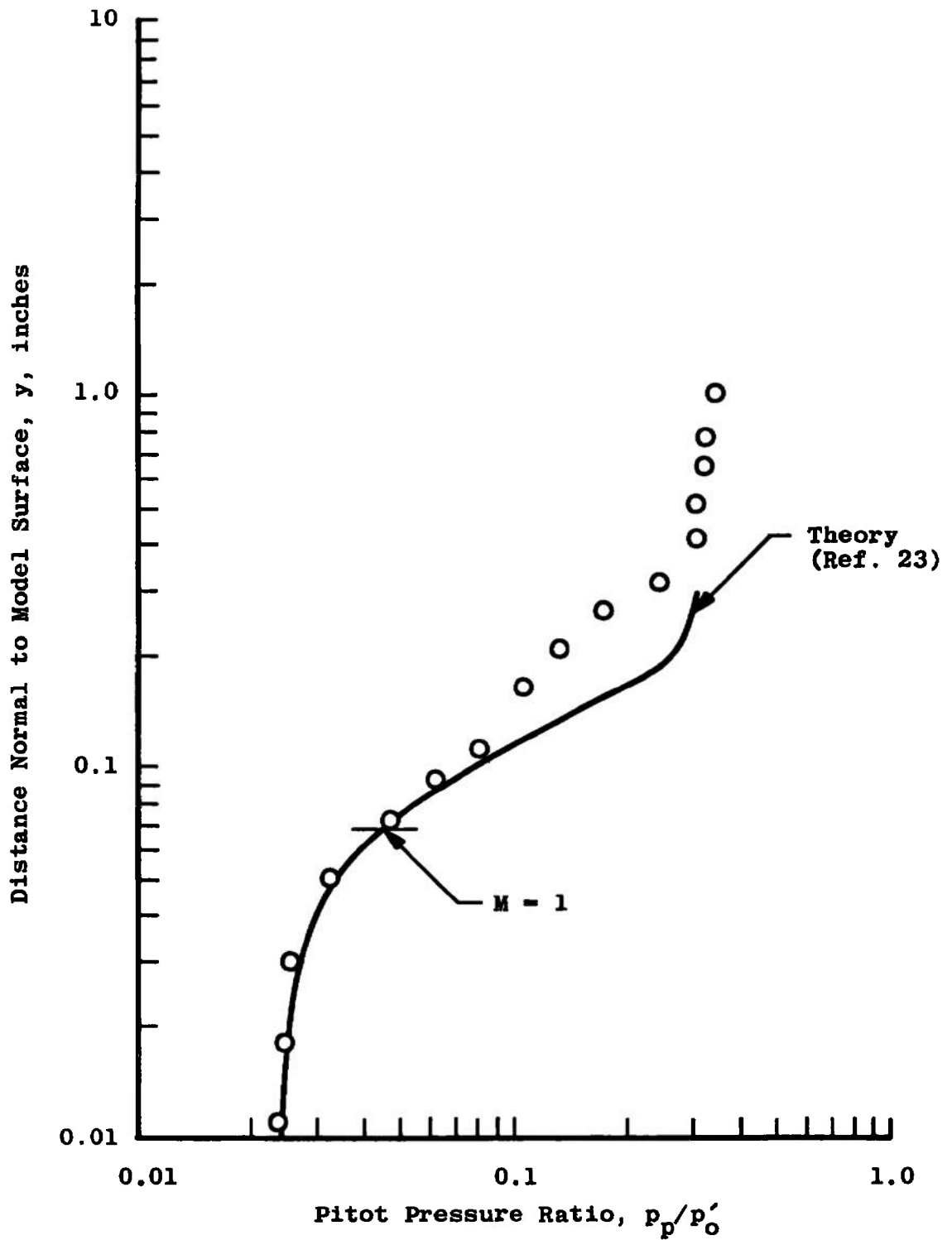


c. Compound Sphere-Cylinder,  $x_p = 25.15$  inches  
 Fig. 14 Concluded

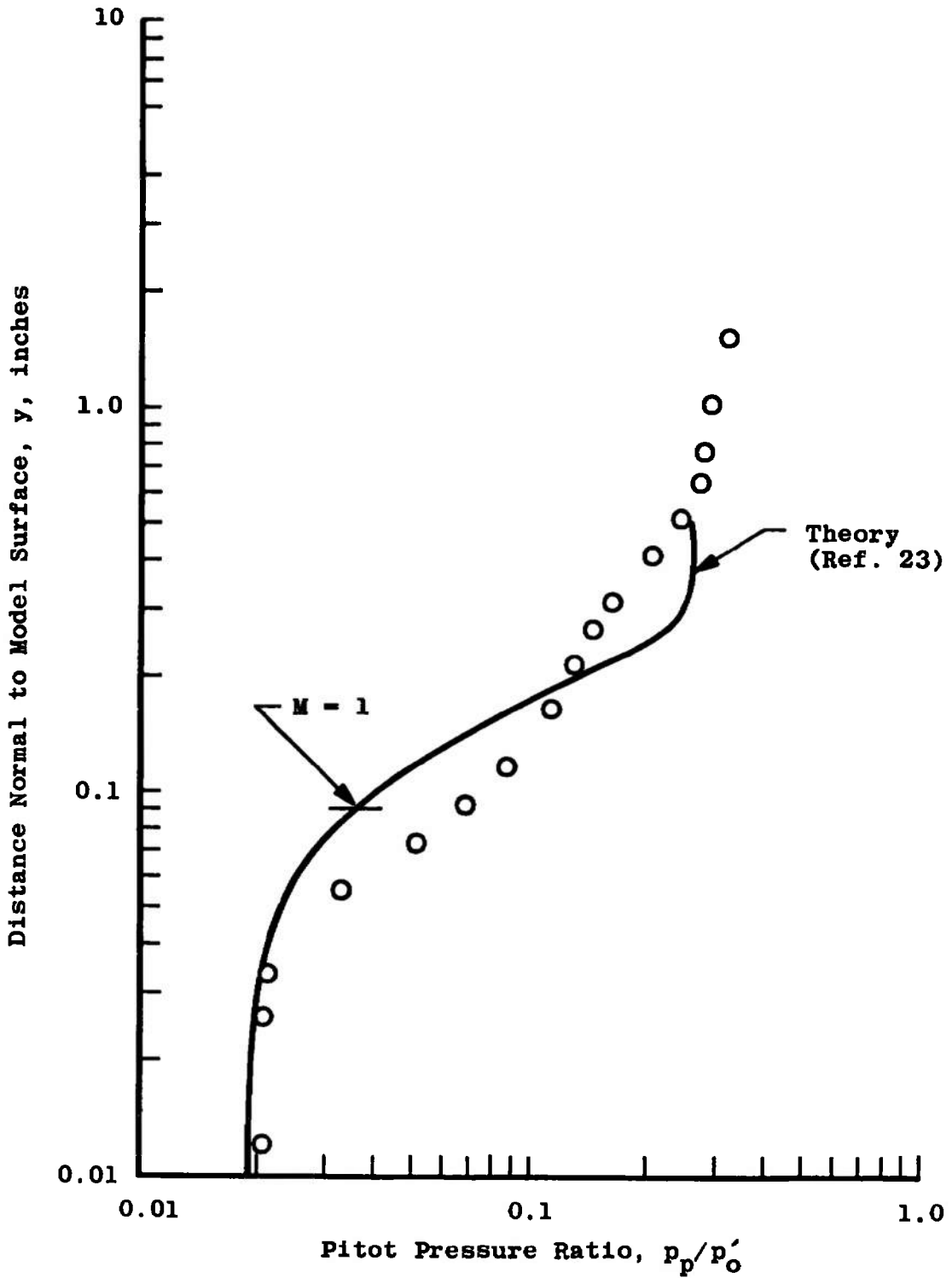


a.  $(x_p - x_k) = 2.88$

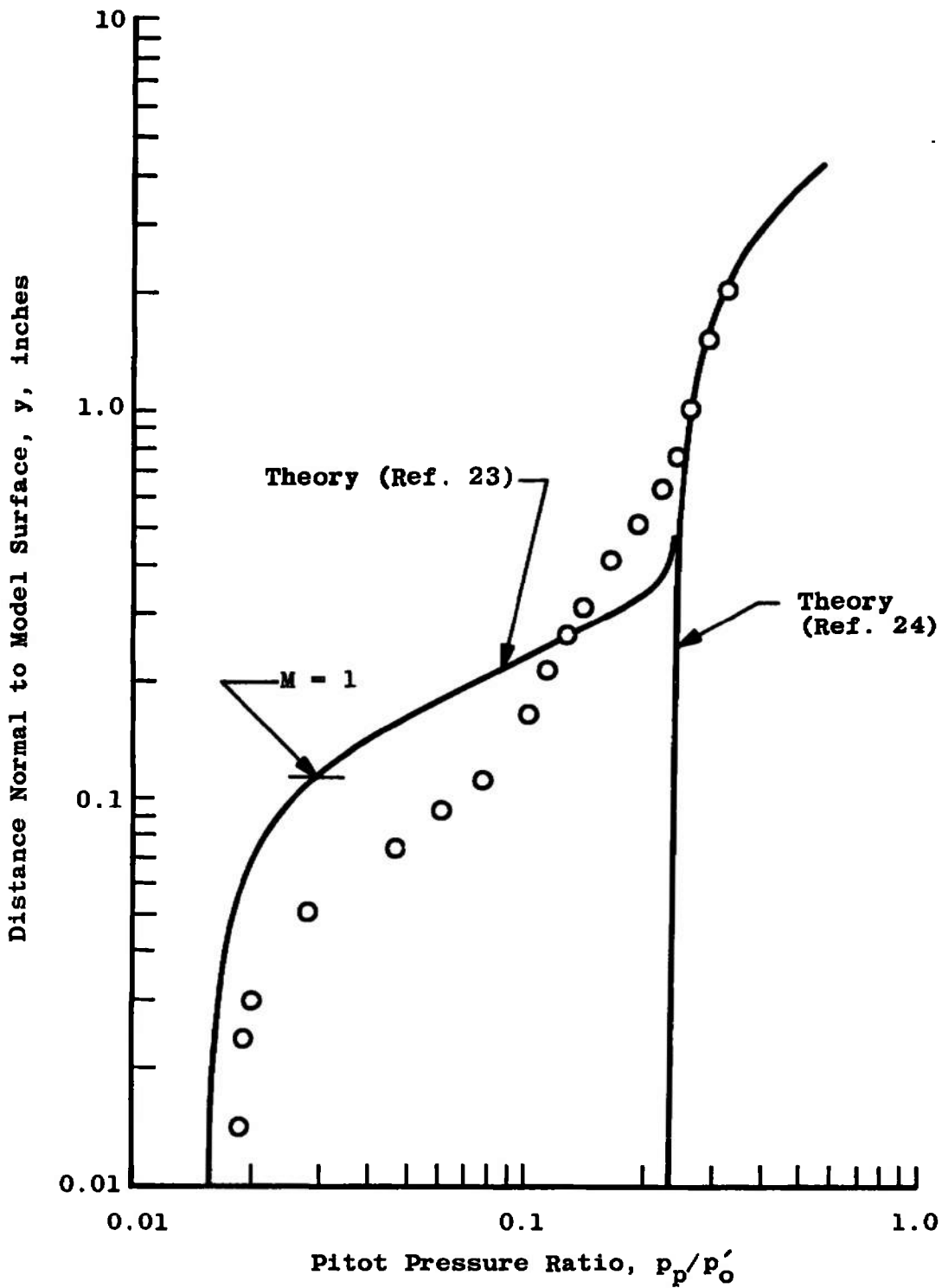
Fig. 15 Effect of Boundary Layer Trips ( $k = 0.125$  inches,  $x_k = 4.73$  inches) on the Development of Pitot Pressure Profiles for the Hemisphere-Cylinder at  $M_\infty = 8$ ,  $Re_{x_0}/in. = 0.19 \times 10^6$



b.  $(x_p - x_k) = 8.88$   
 Fig. 15 Continued



c.  $(x_p - x_k) = 14.88$   
 Fig. 15 Continued



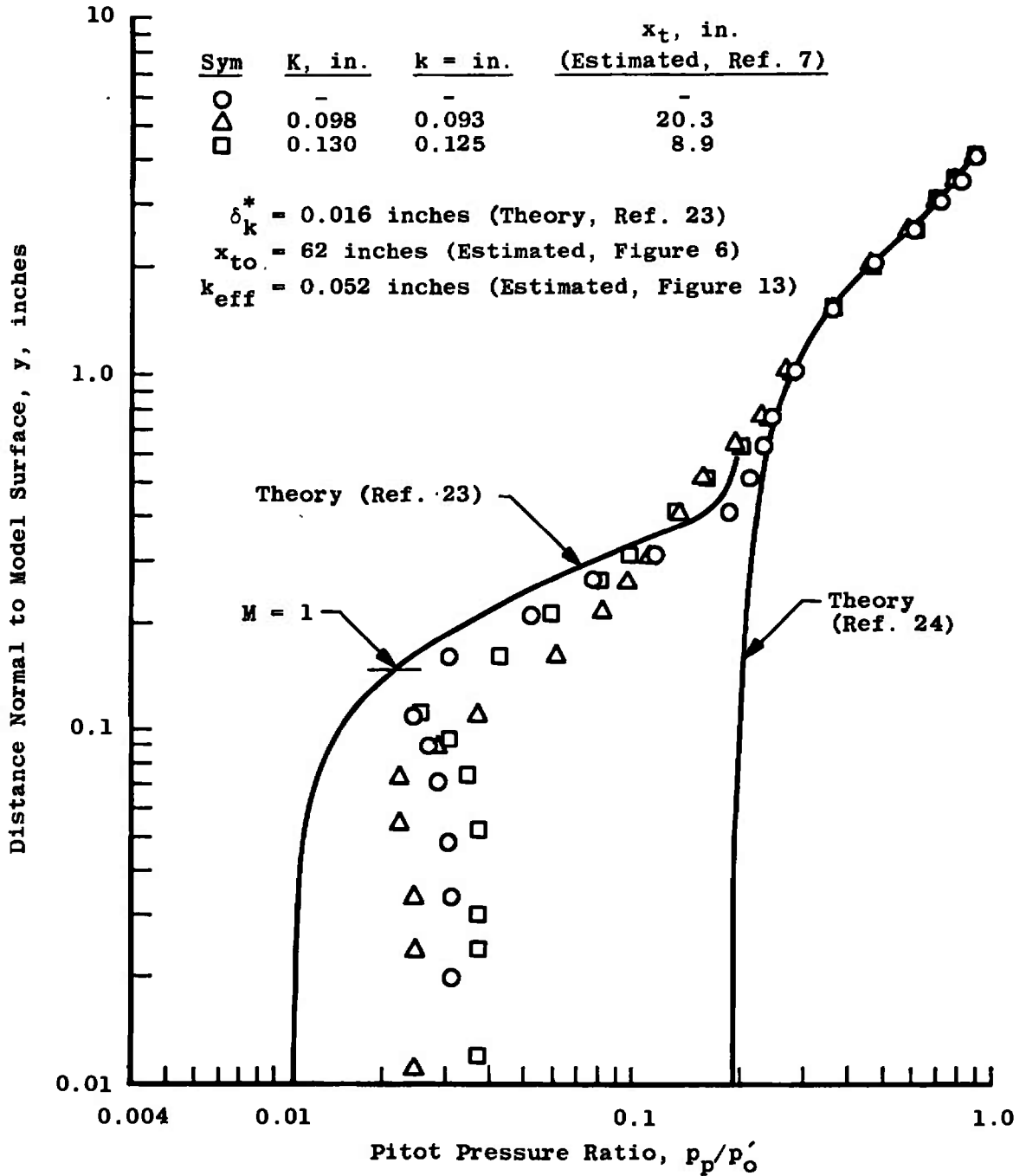
d.  $(x_p - x_k) = 21.06$   
 Fig. 15 Continued

Pitot pressure profiles obtained at the station 14 in. forward of the model base with and without boundary-layer trips are presented in Figs. 16, 17, and 18. The estimated locations of natural boundary-layer transition were obtained by linear extrapolation of the natural transition data obtained at free-stream Mach number 4 (Fig. 6) to the local unit Reynolds numbers at free-stream Mach number 8. This procedure, necessitated by the lack of blunt body transition data at high Mach numbers, is somewhat justified by the insensitivity of the local Mach numbers on blunt bodies to free-stream Mach number changes and also by the limited influence of the Mach number on transition Reynolds numbers for the regime  $2 \leq M_\infty \leq 4$  as discussed previously. On the other hand, the influence of aerodynamic noise, complicated by the presently unknown effects of a strong bow shock wave on the intensity of the radiated noise reaching the model, casts considerable doubt on the validity of such a procedure. Unfortunately, some estimate of the location of natural transition must be made before applying the trip sizing correlation of Potter and Whitfield, and this procedure seemed as reliable as any of the alternatives.

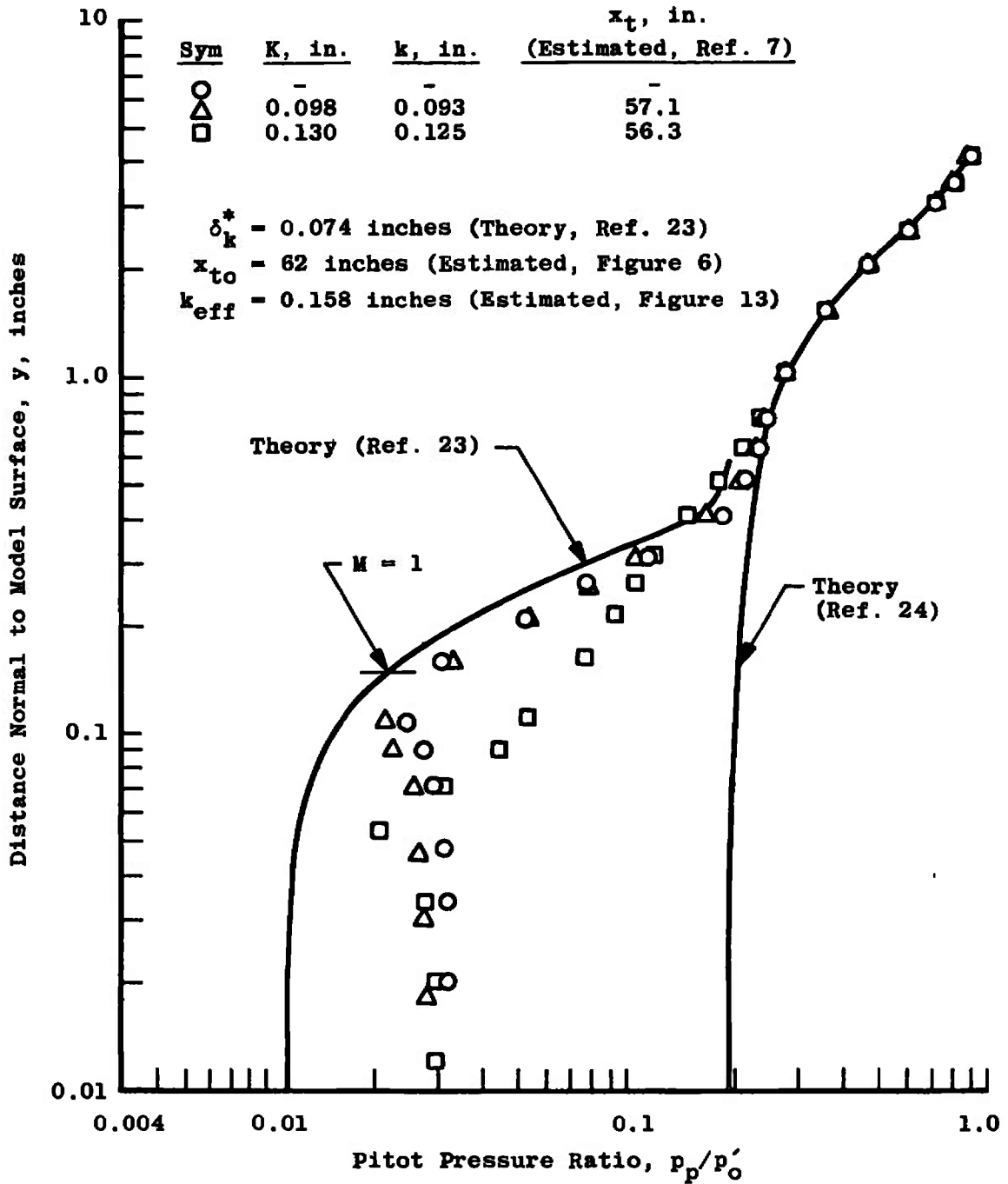
The estimated natural transition distances and theoretical boundary-layer characteristics were used in obtaining the Potter and Whitfield (Ref. 7) predictions of induced transition location listed in Figs. 16 through 18. The critical trip sizes predicted by the correlation of Fig. 13 are also listed in these figures. The predictions are probably in error for the Sphere-Cone-Cylinder with the trip at the sphere-cone junction ( $x_k = 2.17$ , Fig. 16a). It was noted in Section I that locating the trip too near the nose might reduce the trip effectiveness, and these data seem to demonstrate this since the 0.125 trip appeared more effective when located at the cone-cylinder junction ( $x_k = 10.74$  in., Fig. 16b) even though the ratio  $k/\delta^*_k$  was nearly five times greater at the forward location. In other words, in Fig. 16b, the outer portion of the boundary layer appeared to be transitional.

## SECTION V CONCLUDING REMARKS

An investigation was conducted to determine the effectiveness of three-dimensional (spherical) boundary-layer trips in producing turbulent flow on blunt bodies at supersonic speeds. A temperature sensing gage installed in the model surface proved to be a reliable transition detecting device at Mach number 4 but failed to provide satisfactory data at Mach number 8. The investigation of induced transition at higher Mach numbers is continuing with the installation of Gardon heat transfer gages



a.  $x_k = 2.17$  inches (Sphere-Cone Junction).  
 Fig. 16 Pitot Pressure Profiles on the Sphere-Cone-Cylinder at Station  $x_p = 31.80$ ,  $M_\infty = 8$ ,  $Re_\infty/in. = 0.19 \times 10^6$



b.  $x_k = 10.74$  inches (Cone-Body Junction)  
 Fig. 16 Concluded

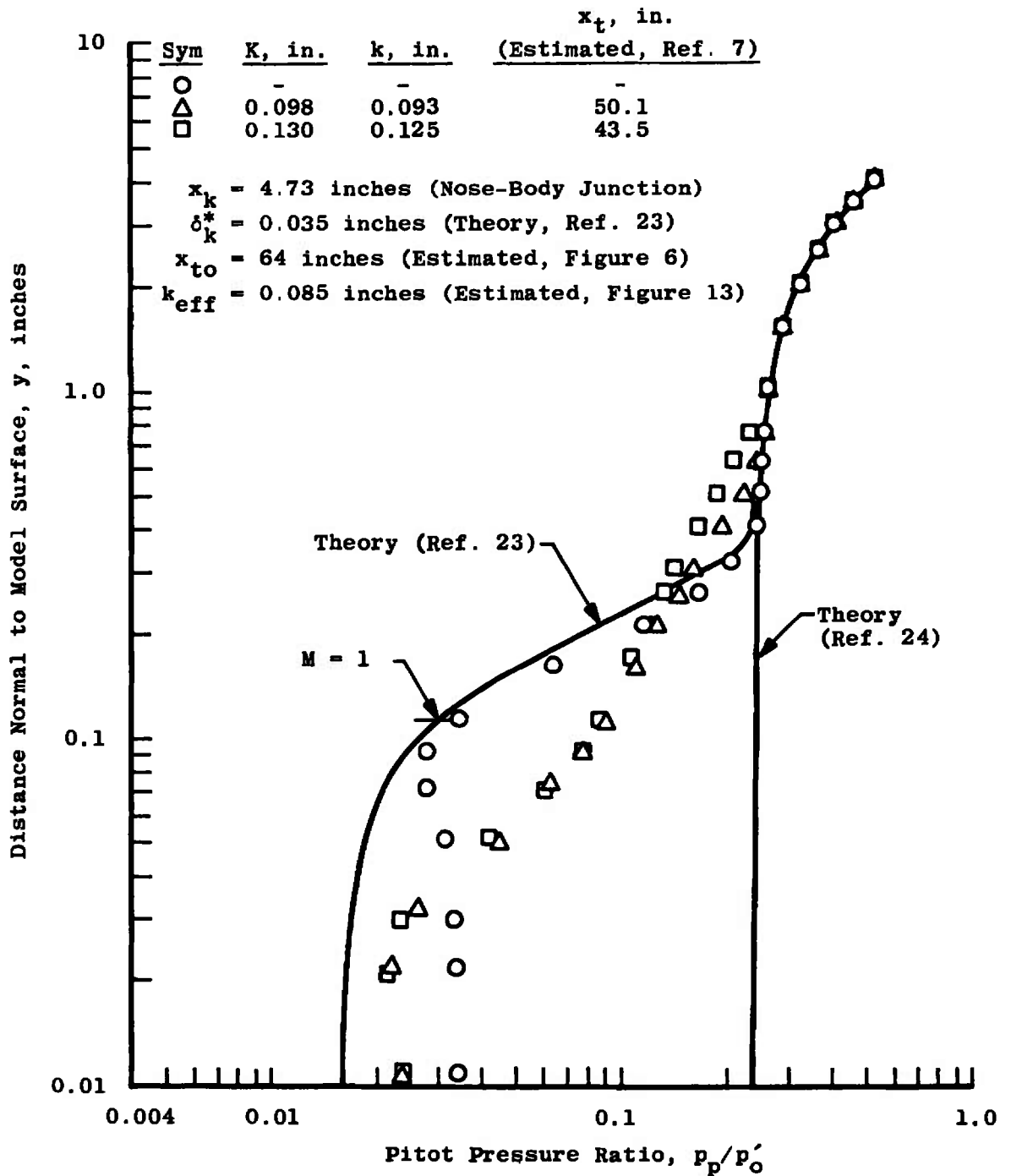


Fig. 17 Pitot Pressure Profiles on the Hemisphere-Cylinder at  $x_p = 25.79$ ,  $M_\infty = 8$ ,  $Re_\infty/in. = 0.19 \times 10^6$

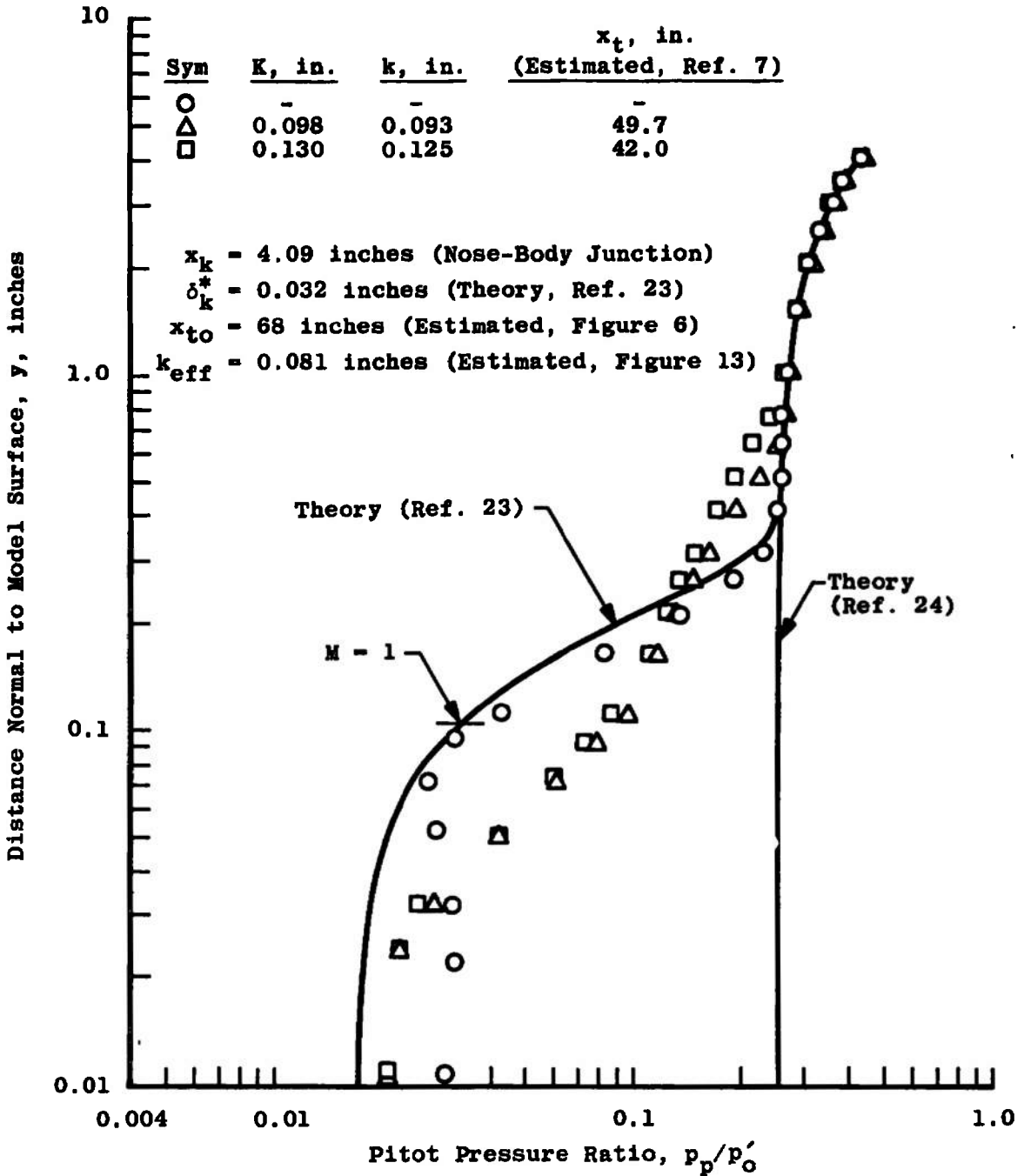


Fig. 18 Pitot Pressure Profiles for the Compound Sphere-Cylinder at  $x_p = 25.15$  inches,  $M_\infty = 8$ ,  $Re_\infty/in. = 0.19 \times 10^6$

(Ref. 27) in the model surface. These gages have been designed especially for operation at the high model temperatures that exist when a model is exposed to a high temperature airstream for extended periods of time.

An empirical modification of a blunt body trip sizing technique proposed by van Driest and Blummer (Ref. 13) was shown to be necessary if a correlation of their original data and the present results at Mach number 4 is to be achieved. However, there is presently no evidence to support the use of the correlation beyond this limited range of experimental conditions and model geometries.

The data are in general agreement with results of the zero pressure gradient trip sizing analysis first proposed by Potter and Whitfield (Refs. 7 and 25) in 1960. Because their method required no modification and predicts the present blunt body results reasonably well, use of the Potter-Whitfield technique for predicting the influence of trips on transition is at the present time considered the best course of action, even for blunt bodies where large pressure gradients exist.

It is felt that the primary objectives of the investigation as outlined in Section I were accomplished, although numerous problems obviously remain. In addition to the testing planned at Mach number 8, further investigation of bodies less blunt than those of the present test is needed to resolve the unknown effect of bluntness-induced entropy gradients on transition. A systematic investigation of the effects of model wall temperature is also essential to the development of a generally applicable blunt body trip sizing technique.

## REFERENCES

1. Klein, E. J. "Application of Liquid Crystals to Boundary-Layer Flow Visualization." American Institute of Aeronautics and Astronautics Paper No. 68-376, AIAA Third Aerodynamic Testing Conference, San Francisco, California, April 8-10, 1968.
2. Sterrett, J. R., Morrisette, E. L., Whitehead, A. H., Jr., and Hicks, R. M. "Transition Fixing for Hypersonic Flow." National Aeronautics and Space Administration TN-D-4129, Langley Research Center, Langley Station, Hampton, Virginia, October 1967.

3. Holloway, P. F. and Morrisette, E. L. "Roughness Effects on Boundary-Layer Transition for Blunt-Leading-Edge Plates at Mach 6." National Aeronautics and Space Administration TN-D-3517, Langley Research Center, Langley Station, Hampton, Virginia, August 1966.
4. Pate, S. R. and Schueler, C. J. "Radiated Aerodynamic Noise Effects on Boundary Layer Transition in Supersonic and Hypersonic Wind Tunnels." AIAA Journal, Vol. 7, March 1969, pp. 450-458.
5. Van Driest, E. R. and McCauley, W. D. "The Effect of Controlled Three-Dimensional Roughness on Boundary-Layer Transition at Supersonic Speeds." Journal of the Aero/Space Sciences, Vol. 27, April 1960, pp. 261-271.
6. Jackson, M. W. and Czarnecki, K. R. "Investigation by Schlieren Technique of Methods of Fixing Fully Turbulent Flow on Models at Supersonic Speeds." National Aeronautics and Space Administration TN-D-242, Langley Research Center, Langley Field, Virginia, April 1960.
7. Potter, J. L. and Whitfield, J. D. "Effects of Slight Nose Bluntness and Roughness on Boundary Layer Transition in Supersonic Flows." Journal of Fluid Mechanics, Part IV, Vol. 12, 1962, pp. 501-535.
8. Klebanoff, P. S., Schubauer, G. B., and Tidstrom, K. D. "Measurements of the Effect of Two-Dimensional and Three-Dimensional Roughness Elements on Boundary-Layer Transition." Journal of the Aeronautical Sciences, Vol. 22, November 1955, pp. 803-804.
9. Van Driest, E. R. and McCauley, W. D. "The Effect of Controlled Three-Dimensional Roughness on Boundary Layer Transition at Supersonic Speeds." AFOSR-TN-58-176 (AD152209), North American Aviation, Inc., Missile Division, Anaheim, California, November 1958.
10. McCauley, W. D., Saydah, A. R., and Bueche, J. F. "Effect of Spherical Roughness on Hypersonic Boundary-Layer Transition." AIAA Journal, Vol. 4, December 1966, pp. 2142-2148.
11. Van Driest, E. R. and Blummer, C. B. "Boundary Layer Transition at Supersonic Speeds - Three-Dimensional Roughness Effects (Spheres)." AFOSR 1493, North American Aviation, Inc., Space Sciences Laboratory, Anaheim, California, August 1961.

12. Dryden, H. L. "Review of Published Data on the Effect of Roughness on Transition from Laminar to Turbulent Flow." Journal of the Aeronautical Sciences, Vol. 20, July 1953, pp. 477-482.
13. Van Driest, E. R. and Blummer, C. B. "Boundary Layer Transition on Cones and Spheres at Supersonic Speeds - Effects of Roughness and Cooling." AFOSR Scientific Report No. 67-2048, Ocean Systems Operations of North American Rockwell Corporation, Anaheim, California, July 1967.
14. Braslow, A. L., Hicks, R. M., and Harris, R. V., Jr. "Use of Grit-Type Boundary Layer Transition Trips on Wind Tunnel Models." National Aeronautics and Space Administration TN-D-3579, Langley Research Center, Langley Station, Hampton, Virginia, September 1966.
15. Schiller, L. "Strömung in Röhren." Handbuch der Experimentalphysik, Hydro- und Aerodynamik, Ludwig Schiller, editor. Vol. IV, Part 4. Leipzig: Akad, Verlagsgesellschaft m. b. H., 1932, pp. 189-192.
16. Fage, A. "The Smallest Size of a Spanwise Surface Corrugation Which Affects Boundary-Layer Transition on an Aerofoil." Aeronautical Research Council Report No. 2120, London, England, January 1943.
17. Braslow, A. L. "Review of the Effect of Distributed Surface Roughness on Boundary-Layer Transition." Advisory Group for Aeronautical Research and Development Report No. 254, North Atlantic Treaty Organization, Paris, France, April 1960.
18. Braslow, A. L. and Knox, E. C. "Simplified Method for Determination of Critical Height of Distributed Roughness Particles for Boundary Layer Transition at Mach Numbers from 0 to 5." National Advisory Committee for Aeronautics TN-4363, Washington, D. C., September 1958.
19. Braslow, A. L., Knox, E. C., and Horton, E. A. "Effect of Distributed Three-Dimensional Roughness and Surface Cooling on Boundary Layer Transition and Lateral Spread of Turbulence at Supersonic Speeds." National Aeronautics and Space Administration TN-D-53, Langley Research Center, Langley Field, Virginia, October 1959.
20. Potter, J. L. and Whitfield, J. D. "Boundary Layer Transition under Hypersonic Conditions." AGARDograph 97, Part III, presented at AGARD Specialists' Meeting, Naples, Italy, May 10-14, 1965.

21. Whitfield, J. D. and Iannuzzi, F. A. "Experiments on Roughness Effect on Cone Boundary Layer Transition up to Mach 16." AIAA Journal, Vol. 7, March 1969, pp. 465-470.
22. Potter, J. L. and Whitfield, J. D. "The Influence of Slight Leading-Edge Bluntness on Boundary Layer Transition at a Mach Number of Eight." AEDC-TDR-64-18 (AD431533), Arnold Air Force Station, Tennessee, March 1964.
23. Adams, J. C. "Theoretical Boundary Layer Solution in Levy-Lees Variables." Computer Program, Arnold Engineering Development Center, Arnold Air Force Station, Tennessee, January 1969.
24. Inouye, M., Rakich, J. V., and Lomax, H. "A Description of Numerical Methods and Computer Programs for Two-Dimensional and Axisymmetric Supersonic Flow over Blunt-Nosed and Flared Bodies." National Aeronautics and Space Administration TN-D-2970, Ames Research Center, Moffett Field, California, August 1965.
25. Potter, J. L. and Whitfield, J. D. "Effects of Unit Reynolds Number, Nose Bluntness, and Roughness on Boundary Layer Transition." Advisory Group for Aeronautical Research and Development Report No. 256, North Atlantic Treaty Organization, Paris, France, April 1960.
26. Moeckel, W. E. "Some Effects of Bluntness on Boundary Layer Transition and Heat Transfer at Supersonic Speeds." National Advisory Committee for Aeronautics TN-3653, Lewis Flight Propulsion Laboratory, Cleveland, Ohio, March 1956.
27. Hube, K. F. "An Experimental Method for Determining Heat Transfer Distributions on Blunt Bodies at Hypersonic Mach Numbers." AEDC-TR-69-20 (AD689176), Arnold Air Force Station, Tennessee, June 1969.

UNCLASSIFIED

Security Classification

DOCUMENT CONTROL DATA - R & D

(Security classification of title, body of abstract and indexing annotation must be entered when the overall report is classified)

1 ORIGINATING ACTIVITY (Corporate author) Arnold Engineering Development Center Arnold Air Force Station, Tennessee 37389		2a. REPORT SECURITY CLASSIFICATION <b>UNCLASSIFIED</b>	
		2b. GROUP N/A	
3 REPORT TITLE <b>INVESTIGATION OF THE EFFECTS OF NOSE BLUNTNESS ON NATURAL AND INDUCED BOUNDARY-LAYER TRANSITION ON AXISYMMETRIC BODIES IN SUPERSONIC FLOW</b>			
4 DESCRIPTIVE NOTES (Type of report and inclusive dates) <b>Final Report</b>			
5 AUTHOR(S) (First name, middle initial, last name)  <b>Jack D. Coats, ARO, Inc.</b>			
6 REPORT DATE <b>February 1973</b>	7a. TOTAL NO. OF PAGES <b>60</b>	7b. NO. OF REFS <b>27</b>	
8a. CONTRACT OR GRANT NO.  b. PROJECT NO.  c. Program Element <b>65402234</b>  d.		9a. ORIGINATOR'S REPORT NUMBER(S)  <b>AEDC-TR-73-36</b>	
		9b. OTHER REPORT NO(S) (Any other numbers that may be assigned this report) <b>ARO-VKF-TR-70-224</b>	
10 DISTRIBUTION STATEMENT  <b>Approved for public release; distribution unlimited.</b>			
11 SUPPLEMENTARY NOTES  <b>Available in DDC</b>		12 SPONSORING MILITARY ACTIVITY <b>Arnold Engineering Development Center, Air Force Systems Command, Arnold AF Station, Tenn. 37389</b>	
13 ABSTRACT <p>A series of tests has been conducted at free-stream Mach numbers four and eight to determine the effectiveness of three-dimensional boundary-layer trips in promoting transition on very blunt axisymmetric bodies with near equilibrium wall temperatures. Temperature distributions obtained with temperature sensing gages inserted in the model surface were used to locate boundary-layer transition at Mach number four, and qualitative results, based on pitot pressure measurements, were obtained at Mach number eight. A simple modification of a technique proposed by van Driest and Blummer for determining an effective trip size for blunt bodies is shown to yield a correlation applicable to their data on a sphere at Mach number two and the present configurations at Mach number four. The present data are also shown to be in agreement with the two-dimensional zero pressure gradient trip sizing correlation developed by Potter and Whitfield which has the distinct advantage of providing not only the necessary trip size but also the resulting location of boundary-layer transition.</p>			

14. KEY WORDS	LINK A		LINK B		LINK C	
	ROLE	WT	ROLE	WT	ROLE	WT
blunt bodies boundary-layer transition supersonic flow wind tunnels						

AFPC  
Arnold AFB Tex